



HL-LHC Sextupole Magnet Design Review

Giovanni Volpini
on behalf of the LASA team
with the help of Paolo Fessia

CERN, May 26th, 2015

The electromagnetic design of the sextupole is now finished and the detailed mechanical design is close to its completion.

Following the good results of a preliminary test, we are about to start the manufacture of the sextupole superconducting coils at LASA lab, INFN Milano, Italy.

Before starting the construction, Paolo Fessia and myself have agreed to ask for an independent assessment of the design.

We ask you to express to the two of us (this is an informal review) your comments and criticism, both during this meeting and later, if possible, with an email from each of you.

We will summarize your remarks along with our comments and actions in response to, and send it back to you.

Your kind collaboration is warmly acknowledged!

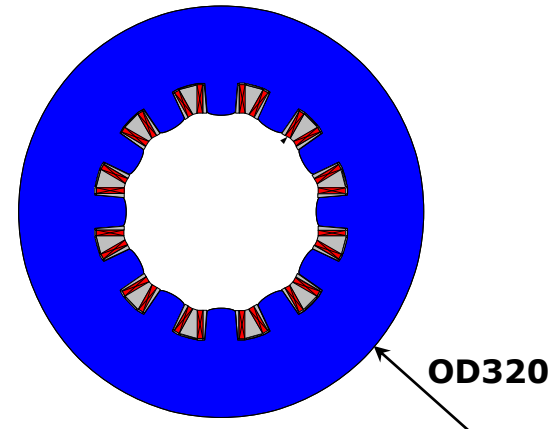
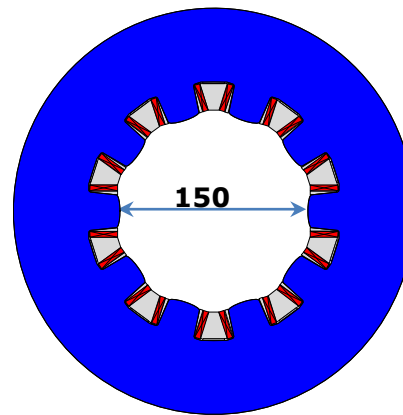
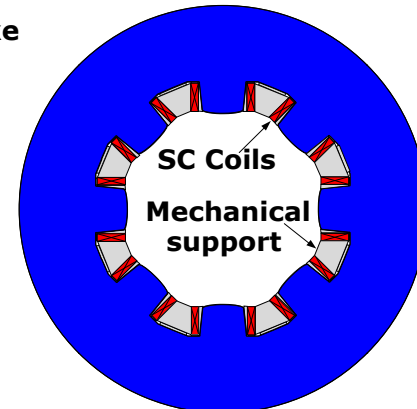
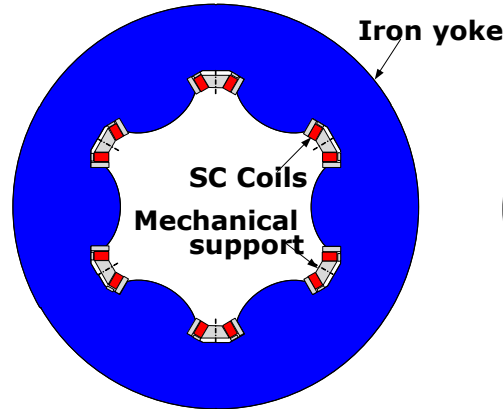
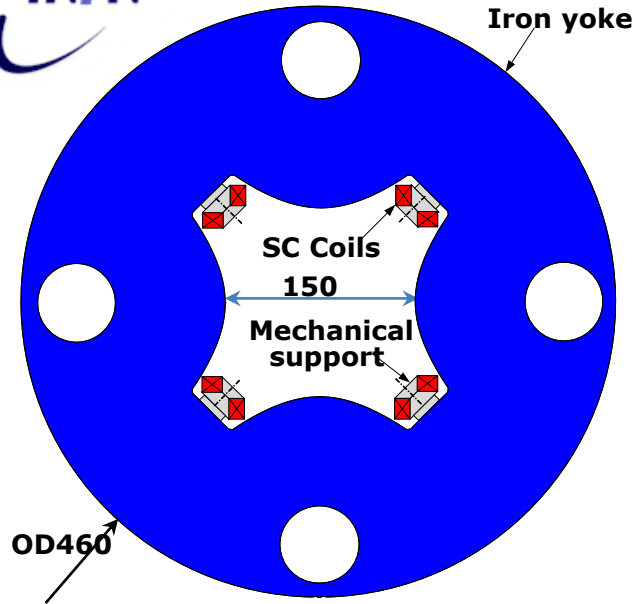
Summary

1. Corrector Magnets Features & Framework
2. Electromagnetic Design & Protection
3. Mechanical Design
4. Superconductor & Coil Manufacture
5. Single Coil Test @ LASA
6. Next Steps & Planning



1. Corrector Magnets Features & Framework

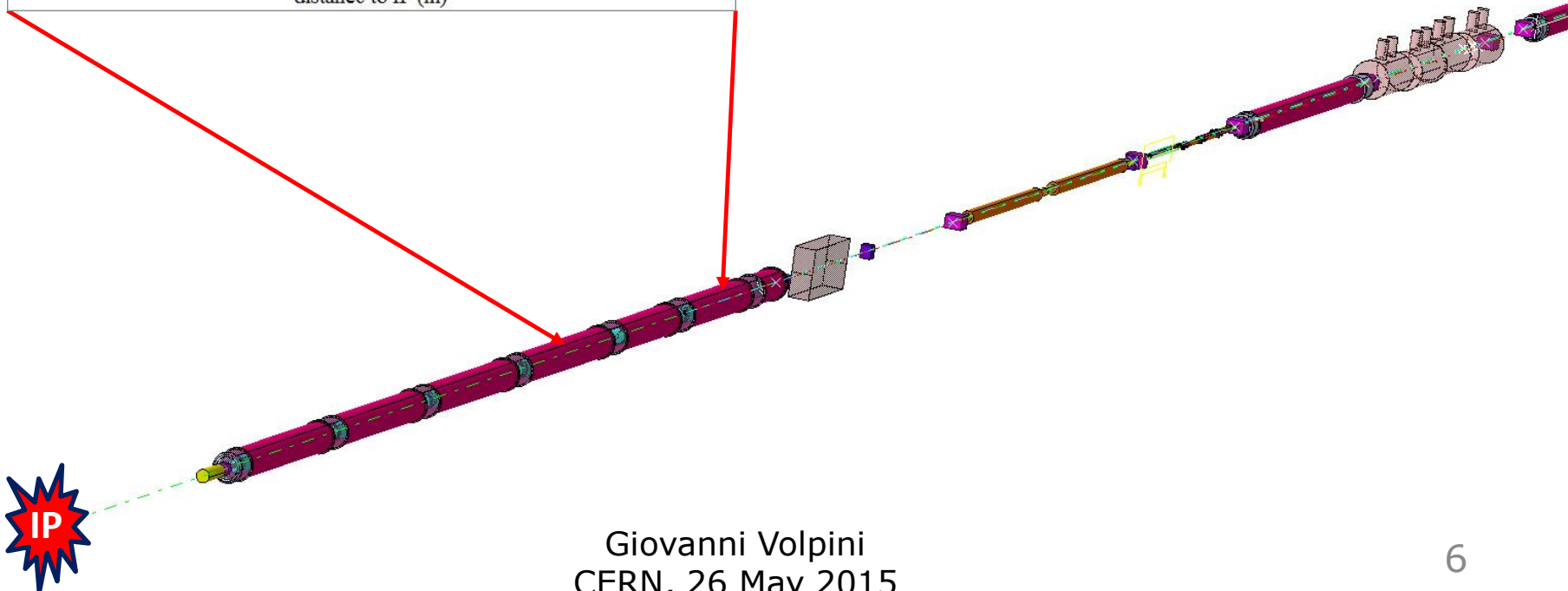
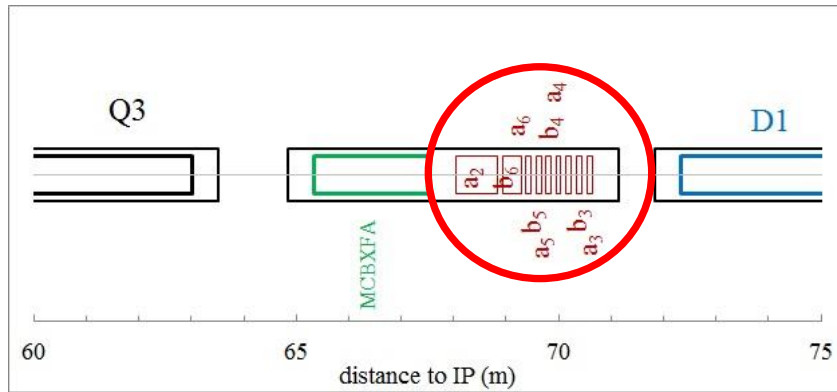
Corrector magnet inventory



From 6-pole to 12-pole magnets exist in both normal and skew form (the latter is shown)

The superferric design was chosen for ease of construction, compact shape, modularity, following the good performance of earlier corrector prototype magnets developed by CIEMAT (Spain).

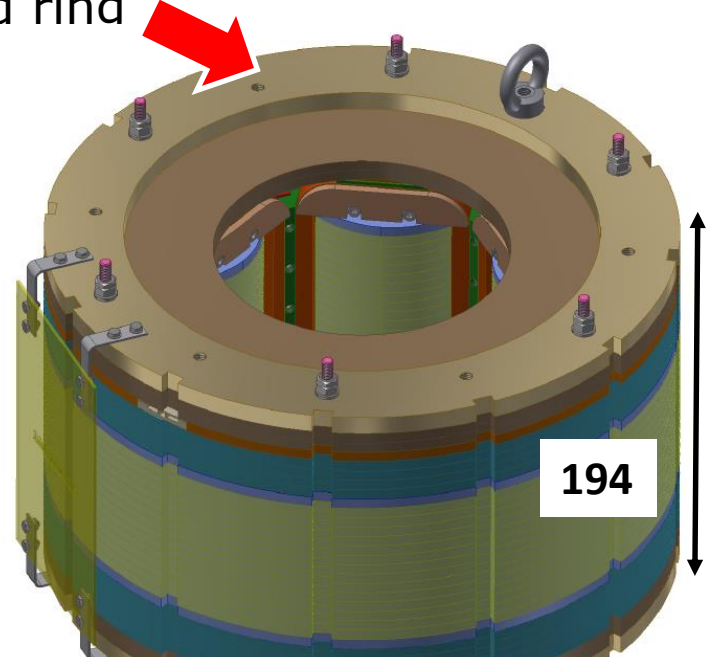
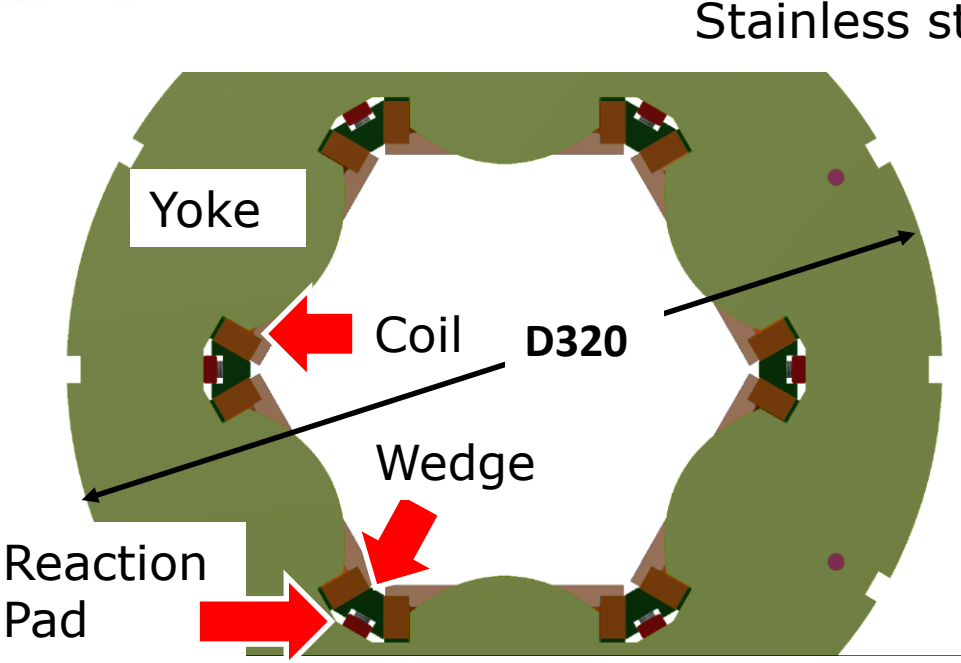
IR layout



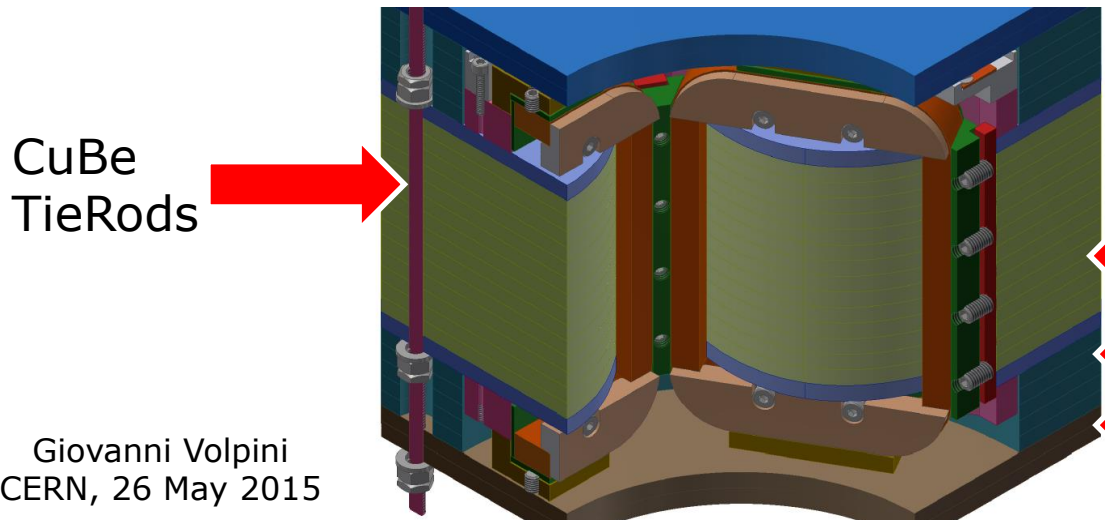
LHC vs. HL-LHC corrector magnet comparison chart

Order	Type	LHC				HL-LHC							
			Aperture	Stored energy	Operating Current	Inductance	Aperture	Stored energy	Operating Current	Integrated field at r=50 mm	Magnetic Length	Differential Inductance @ Iop	
			mm	[J]	[A]	[mH]	[mm]	[kJ]	[A]	[T.m]	[m]	[H]	
2	S	MQSX	70	2,116	550	14	150	24.57	182	1.00	0.807	1.247	
3	N	MCSX	MCSTX	70	39	100	4.7	150	1.28	132	0.06	0.111	0.118
3	S	MCSSX		70	6	50	7.8	150	1.28	132	0.06	0.111	0.118
4	N	MCOX	MCSEX	70	16	100	4.4	150	1.41	120	0.04	0.087	0.152
4	S	MCOSX		70	22	100	3.2	150	1.41	120	0.04	0.087	0.152
5	N							150	1.39	139	0.03	0.095	0.107
5	S							150	1.39	139	0.03	0.095	0.107
6	N	MCTX	MCSTX	70	94	80	29.2	150	4.35	167	0.086	0.430	0.229
6	S							150	0.92	163	0.017	0.089	0.052

Sextupole layout



5.8 mm thick iron laminations, machined by laser cut followed by EDM on the relevant surfaces.



- Yoke
- Bridge
- Flux-return plates

MAGIX & INFN participation to HL-LHC

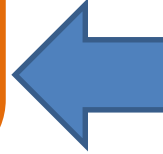
MAGIX

WP1	CORRAL	Design, construction and test of the five prototypes of the corrector magnets for the HL interaction regions of HiLUMI
WP2	PADS	2D & 3D engineering design of the D2 magnets
WP3	SCOW-2G	Development of HTS coil for application to detectors and accelerators
WP4	SAFFO	Low-loss SC development for application to AC magnets

CERN-INFN Collaboration Agreement

Approved by the INFN Board of Directors & signed by INFN President on June 2014; signed by CERN DG on July 17th.

CERN endorses MAGIX WP1 & WP2 deliverables and milestones, contributing with 527 k€



1

2



INFN already involved in FP7-HiLumi (**UE-HILUMI**, GrV)
 WP2 beam dynamics, LNF
 WP3 magnets, MI-LASA
 WP6 cold powering, MI-LASA

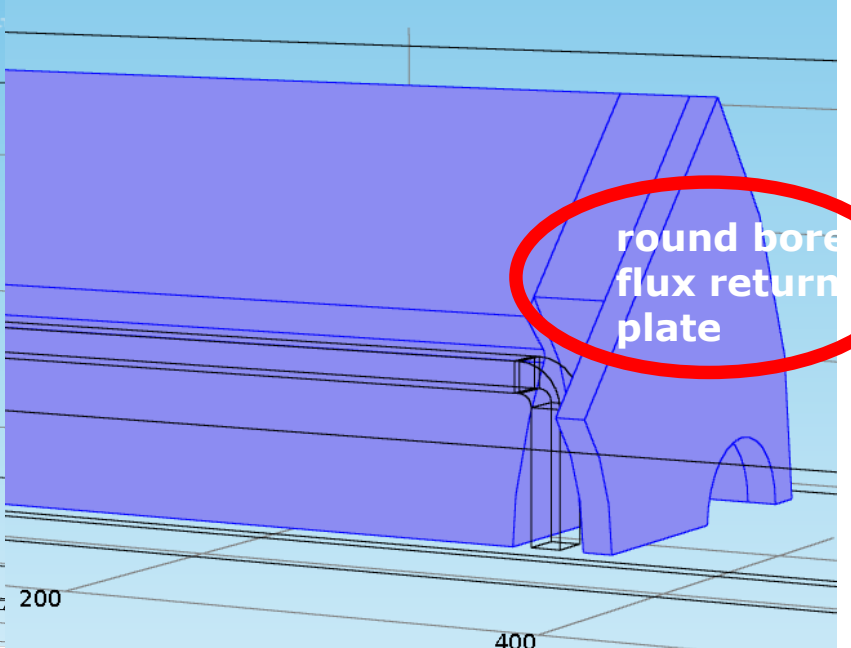
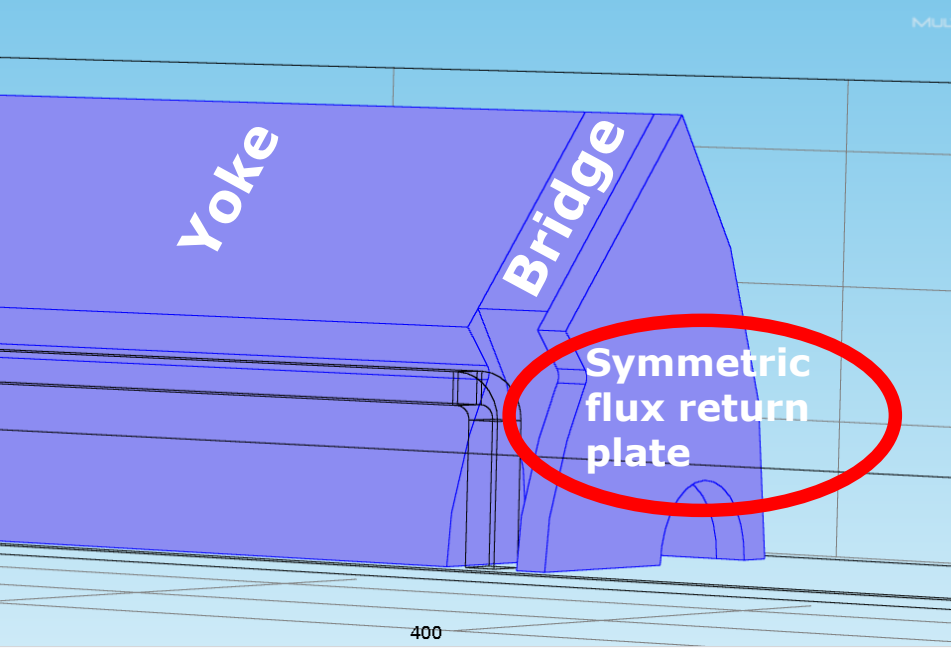
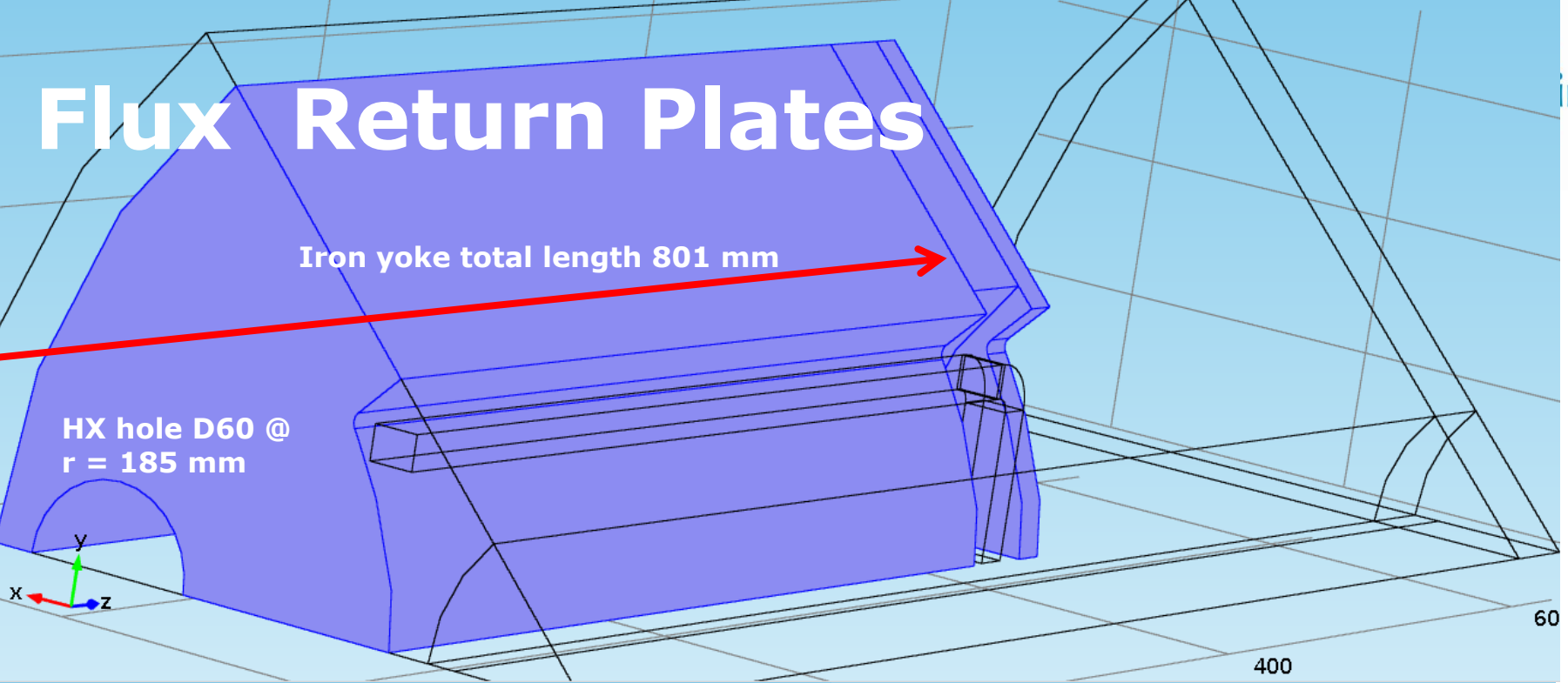
MAGIX is a INFN-funded research project, (GrV, «Call») whose goal is to develop superconducting technologies for application to future accelerator magnets. It includes four WP's, two of which are relevant to HL-LHC
 2014-2017, 1 M€ + personnel funds

2. Electromagnetic Design: Fields and protection

Flux Return Plates

Iron yoke total length 801 mm

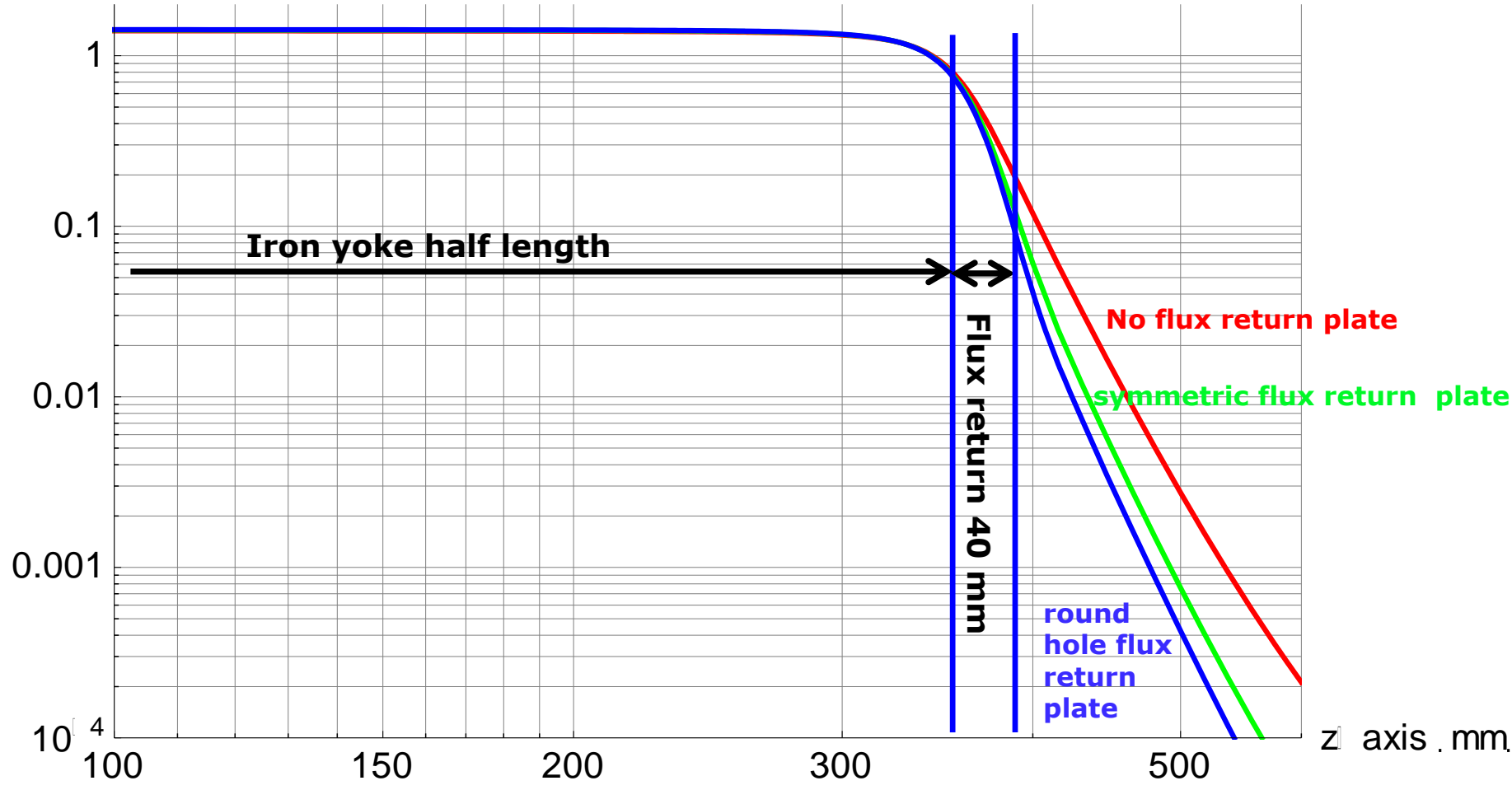
HX hole D60 @
r = 185 mm



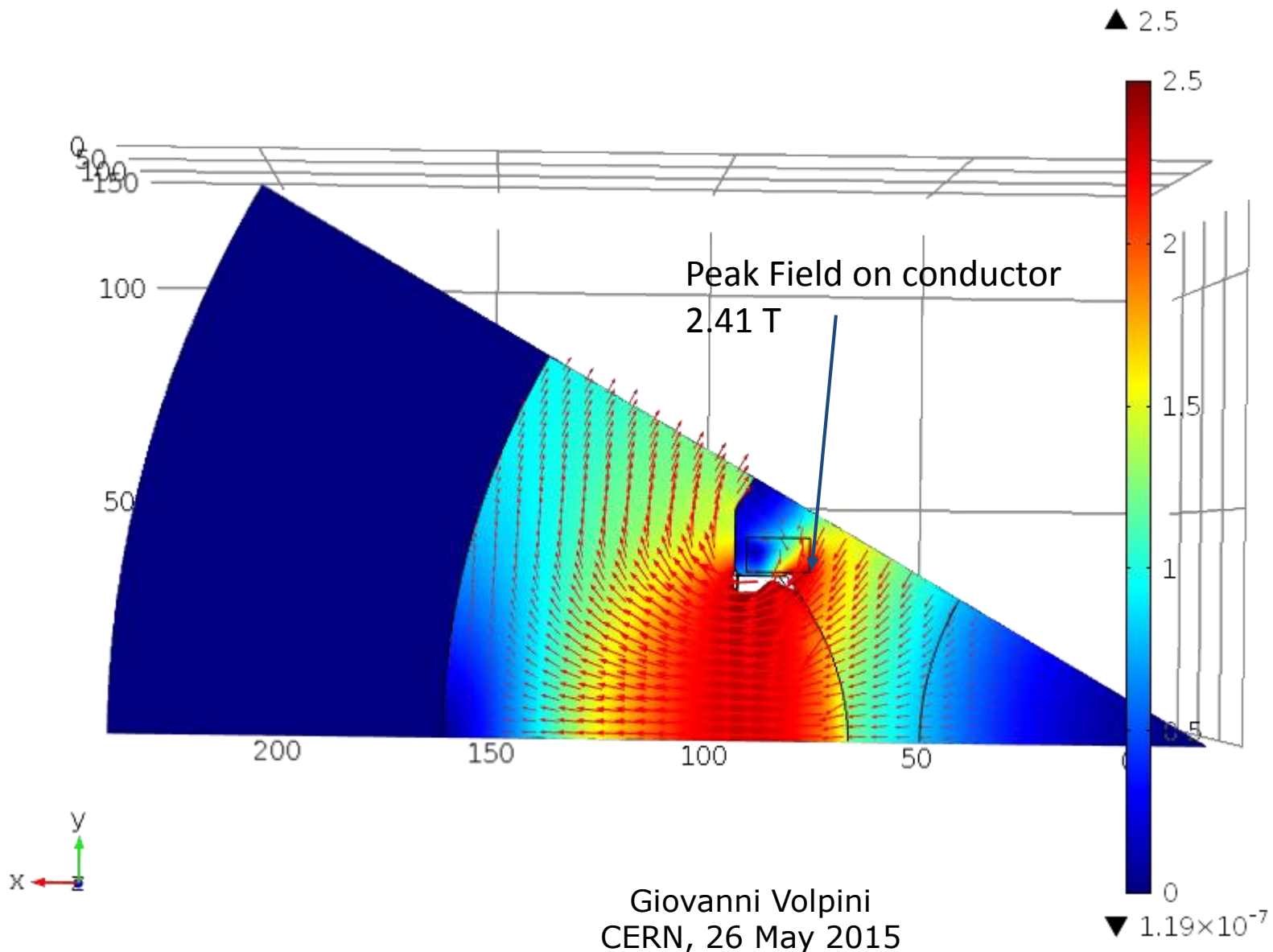
Quadrupole Fringe field for different choices for the flux return plate

A_2 component | integrated strength | 1. Tm

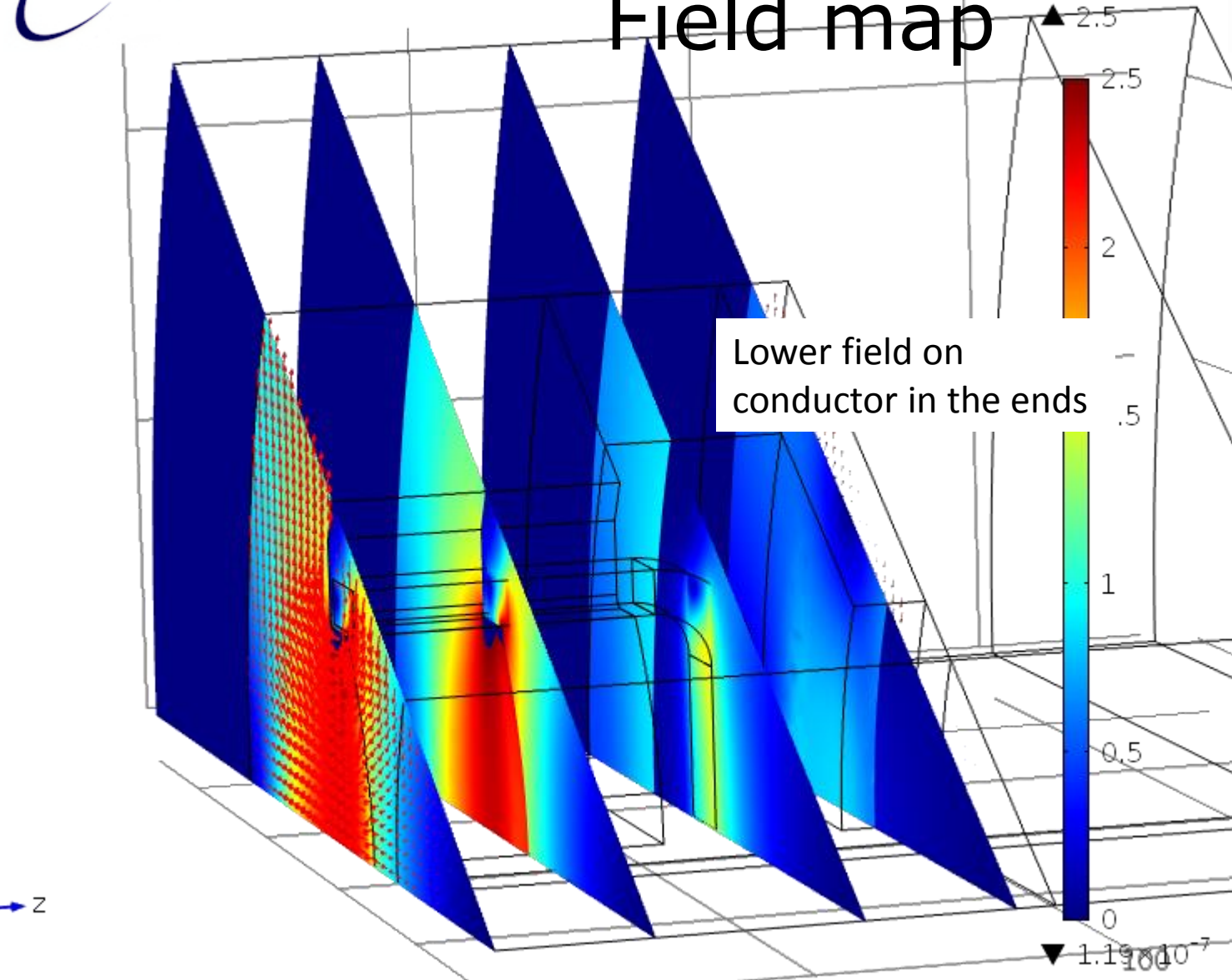
A_2 | r | 50 mm | T.



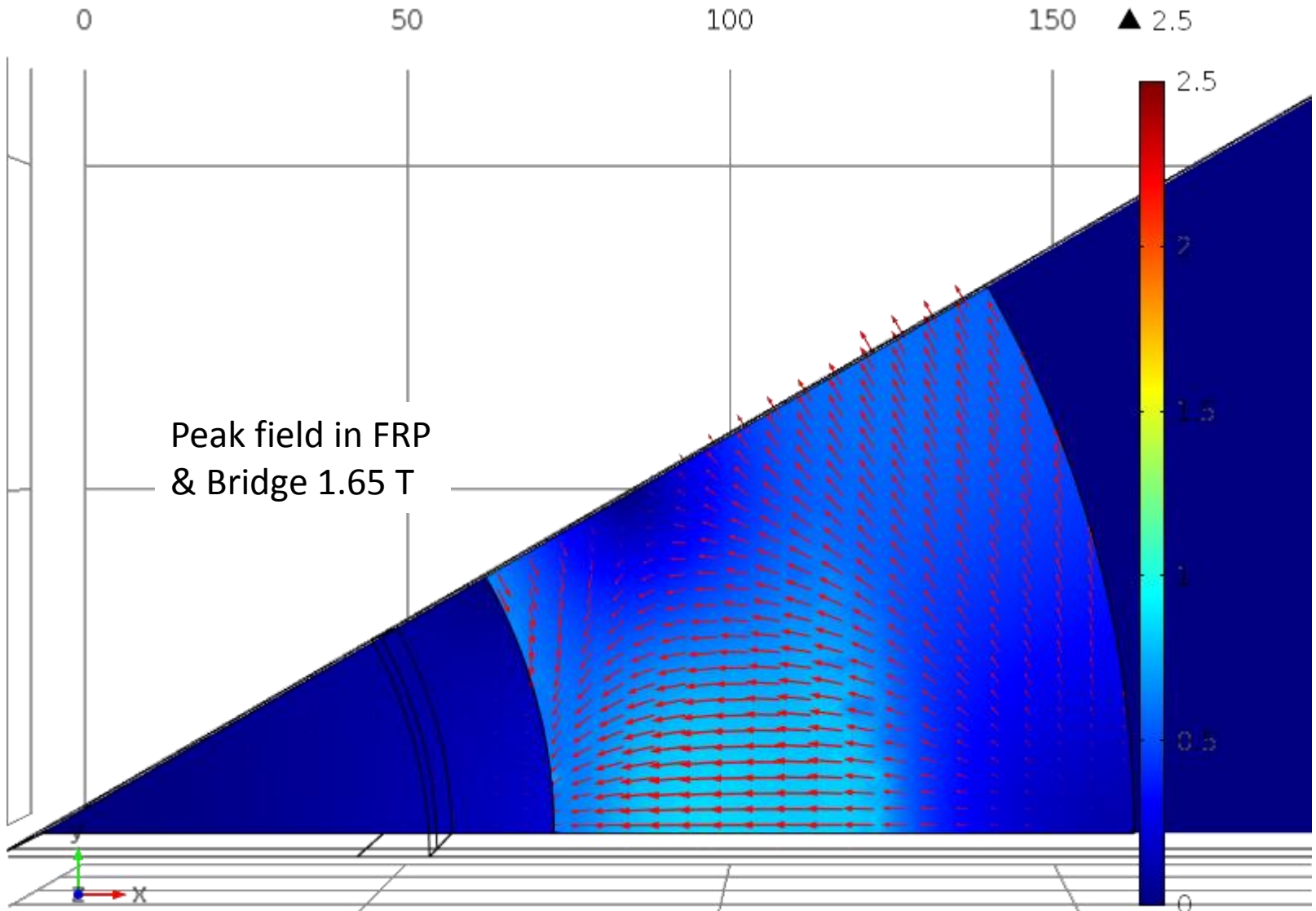
Field map



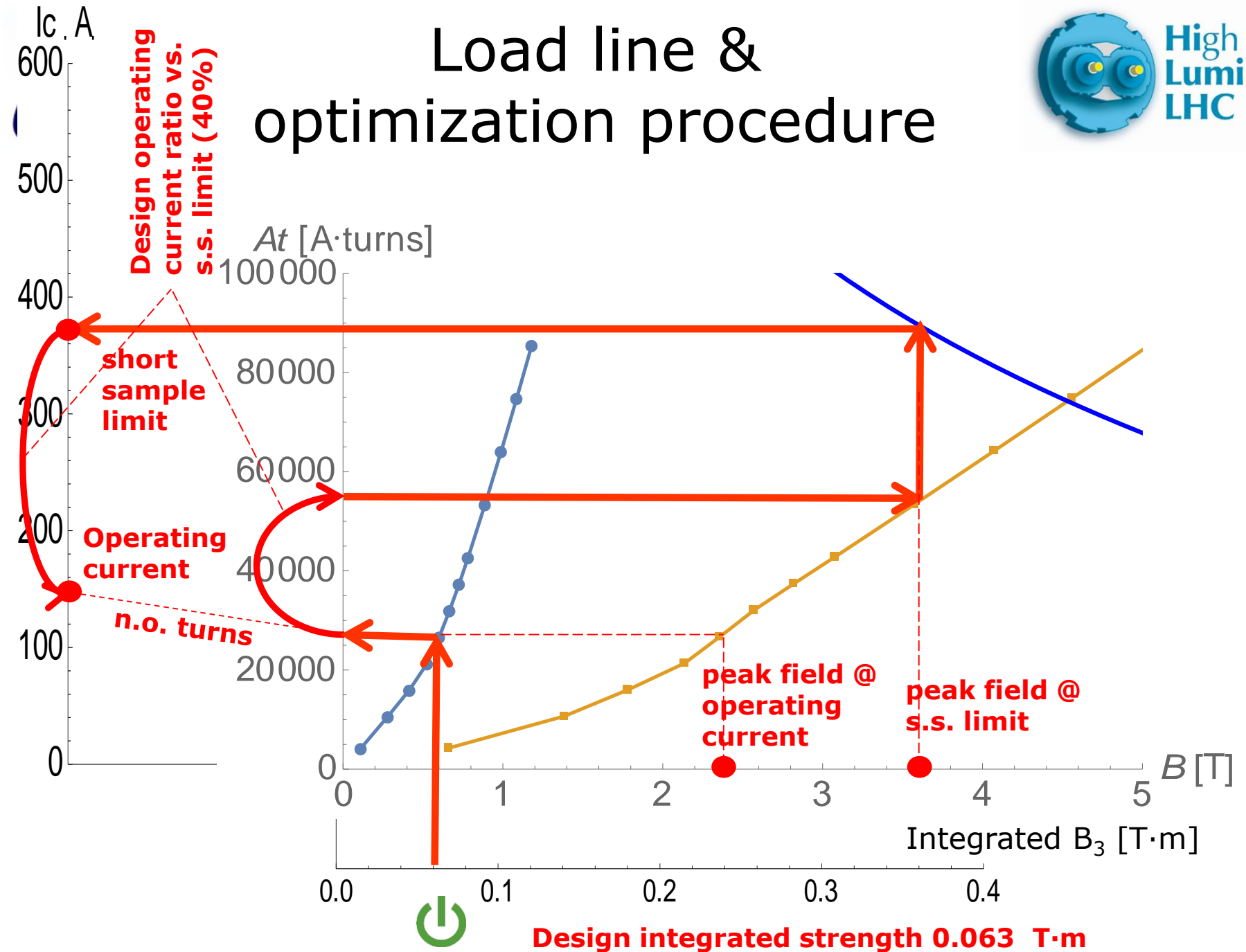
Field map



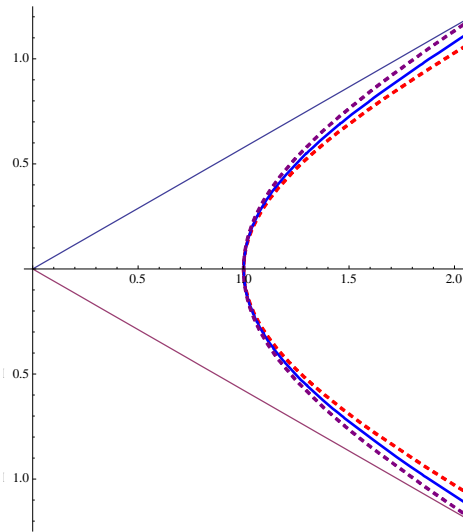
Field in the FRP




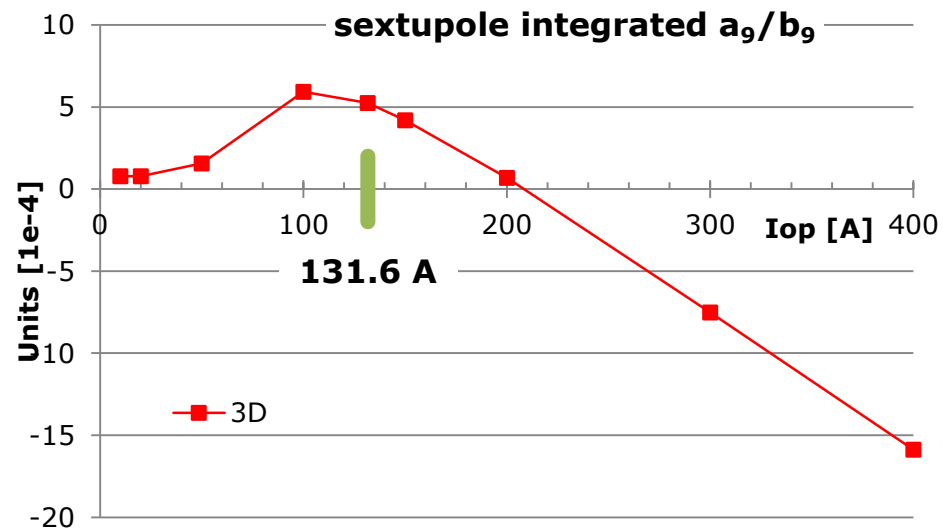
Load line & optimization procedure




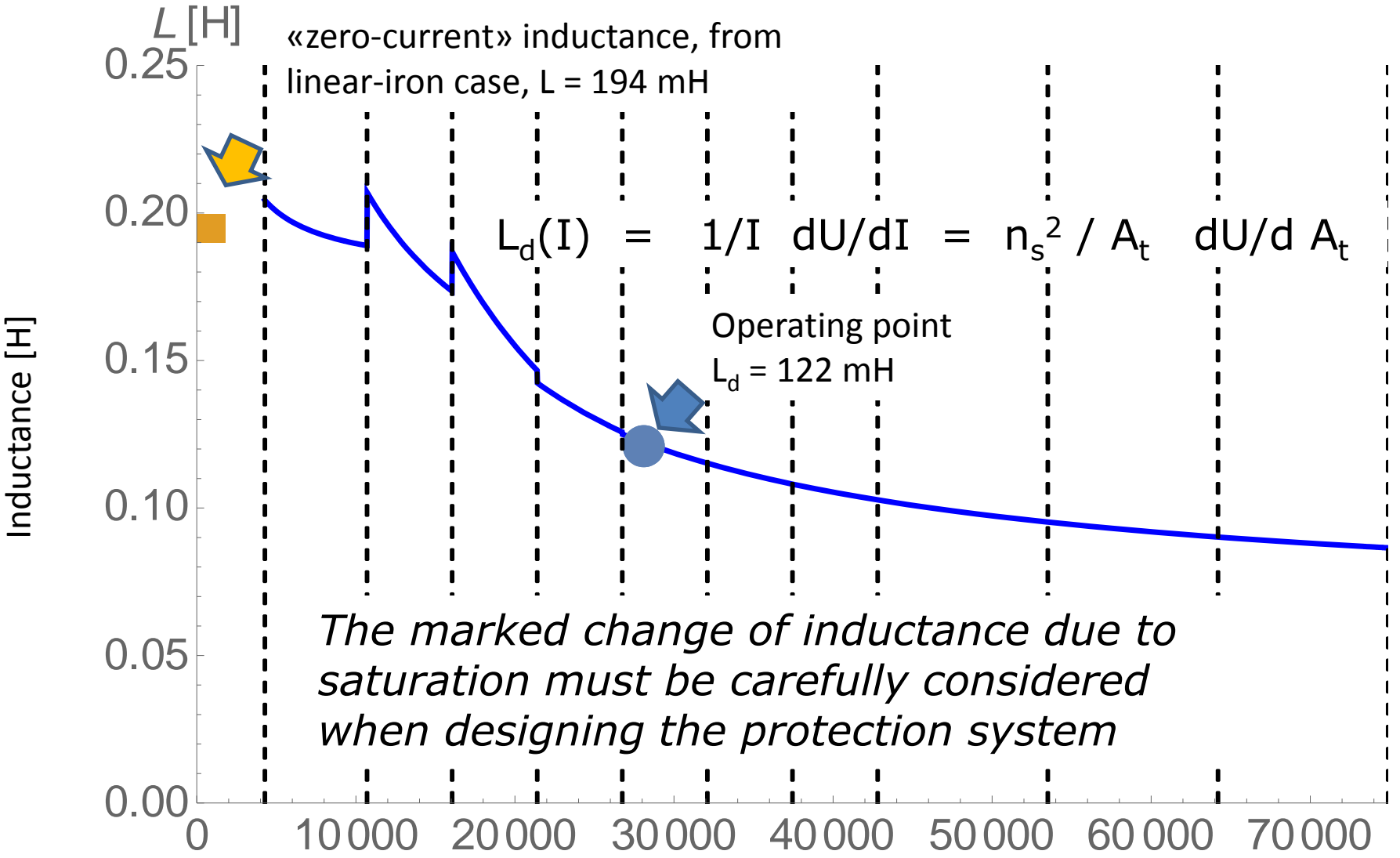
Field Optimization




Geometrical harmonics are controlled by modifying the pole profile, starting from an hyperbolic profile (continuous line), until the first allowed harmonics is < 1 unit.




 No special action has been taken to control **saturation harmonics**, which remain below 6 units on the whole operating range. Here shown a_9/b_9 , others < 1 unit.



Quench protection is based on an external resistor dump, without quench heater, quench detection and switch operation time neglected;

The peak temperatures are computed in two limiting case: $v_{\text{quench}} \rightarrow 0$ (worst case) and $v_{\text{quench}} \rightarrow \infty$, limiting the quench to one coil only;

n	$I_{\text{op}}[\text{A}]$	Tmax[K]		$R_{\text{coil}} [\Omega]$		$R_{\text{dump}} [\Omega]$
		$v_{\text{quench}} \rightarrow \infty$	$v_{\text{quench}} \rightarrow 0$			
2	300	119.4	>300	7.48	>>	1.000
3	150	49.3	58.7	0.332	<	0.667
4	150	37.8	39.3	0.089	<<	0.667
5	150	35.9	36.9	0.065	<<	0.667
6	150	76.9	243.5	1.757	>	0.667

Warning:
 A somewhat old computation,
 likely to improve with updated figures

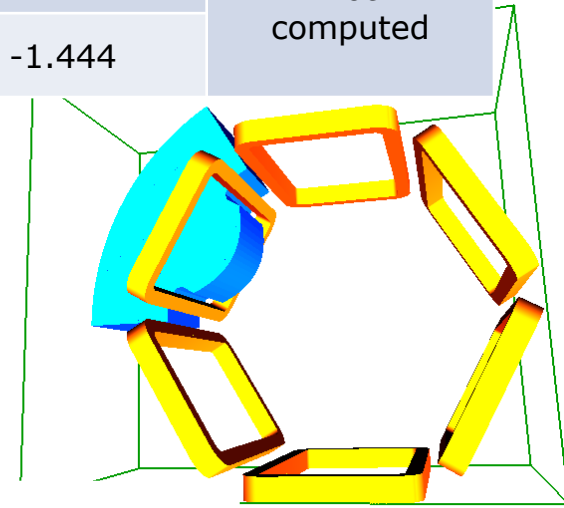
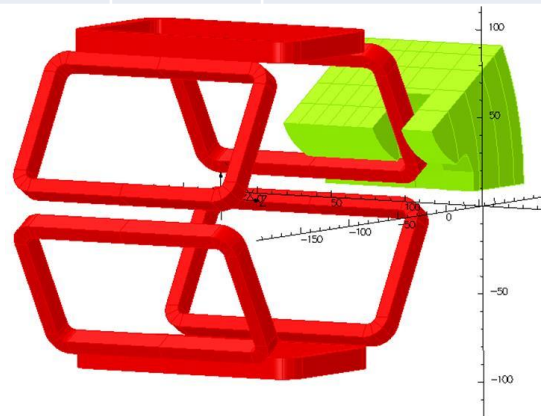
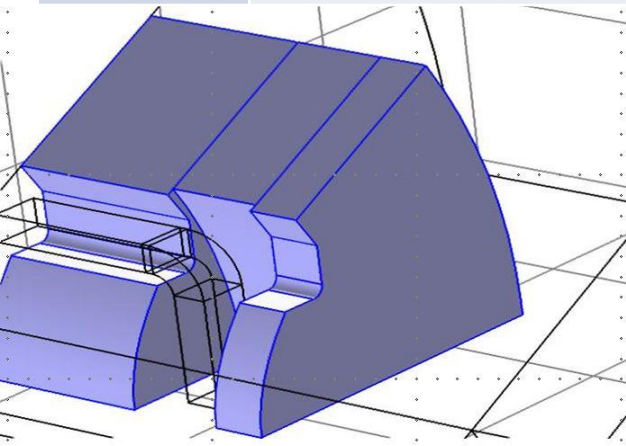
conclusion: quench does not seem a critical point –not obvious for 4-pole, but likely-; a more detailed quench computation with proper propagation speed has to be performed when the design reaches its final stage.

Use different codes to simulate the same sextupole, to cross-check & validate the results:

- **COMSOL + Mathematica for harmonic analysis**
- **OPERA** (2D and 3D models developed by **Alejandro Sanz-Ull**, **CERN-TE-MS**)
- **Roxie**

2D computations: agreement within few parts/ 10^4 on fields; $\sim 1/10$ of unit on relevant harmonics.

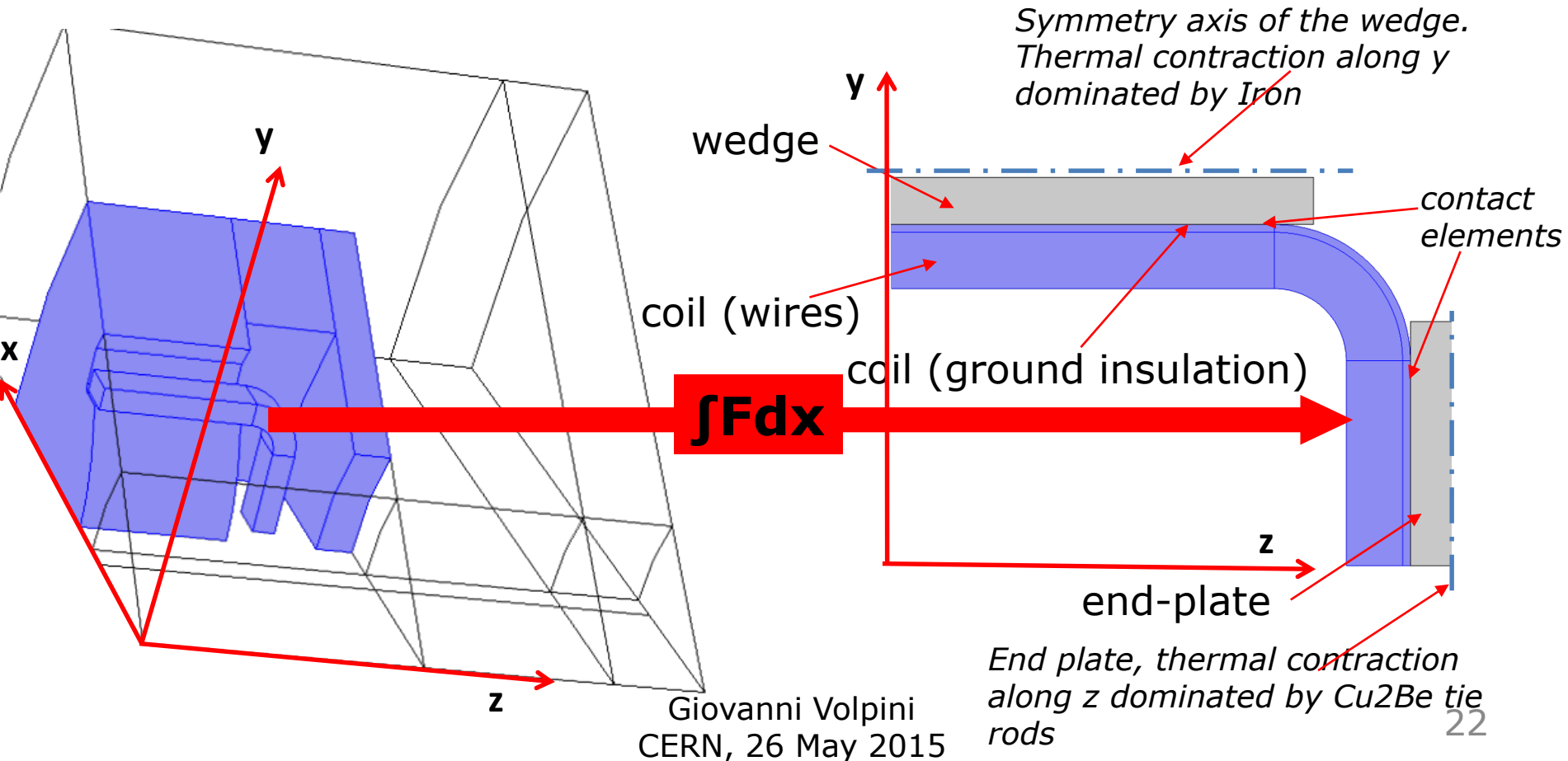
3D computations			COMSOL™	OPERA™	Roxie
No FRY	Integrated B_3 @ $r = 50$ mm	T·m	-0.0758	-0.0759	-0.0756
	b_9	10^{-4}	-21.50	-21.57	-22.5
With FRY	Integrated B_3 @ $r = 50$ mm	T·m	-0.0686	-0.0688	not computed
	b_9	10^{-4}	-1.494	-1.444	



3. Mechanical Design & Assembly Sequence

The electromagnetic 3D model is used to feed volume forces, integrated along the x-direction, to a 2D model of a coil, with wedge and one end-plate.

Although somewhat simplified, we believe it describes the main features; a more detailed model would have been useless since large uncertainties come from mechanical properties of the coils, friction between components, etc.



Mechanical properties

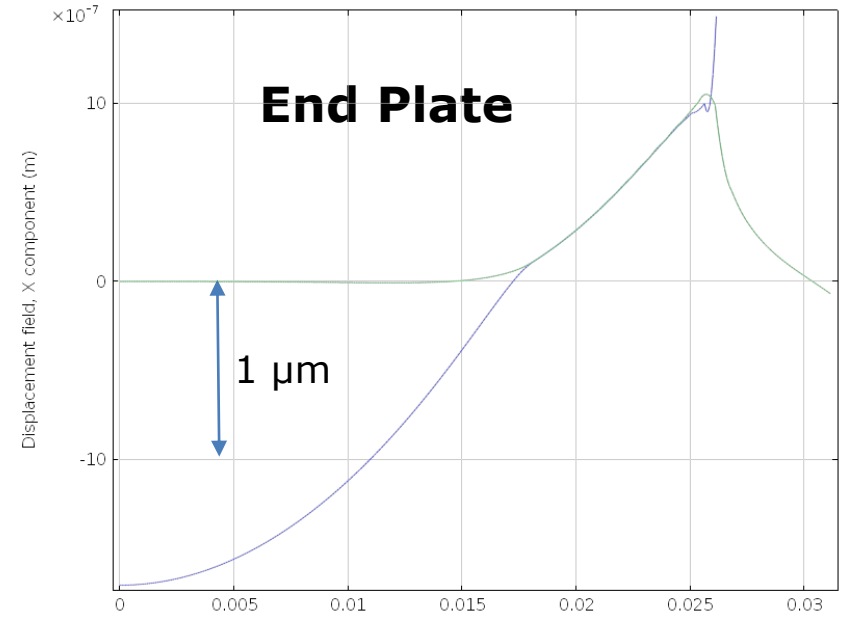
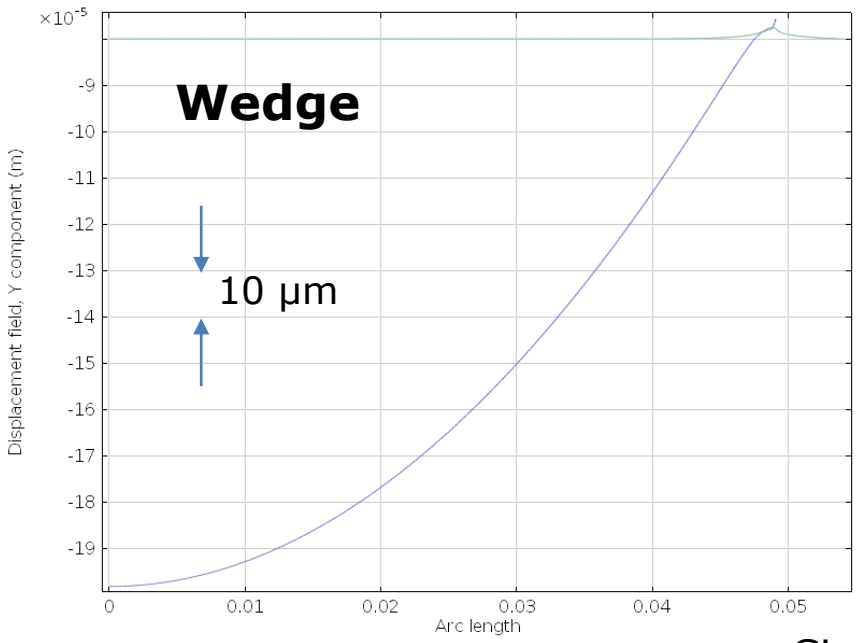
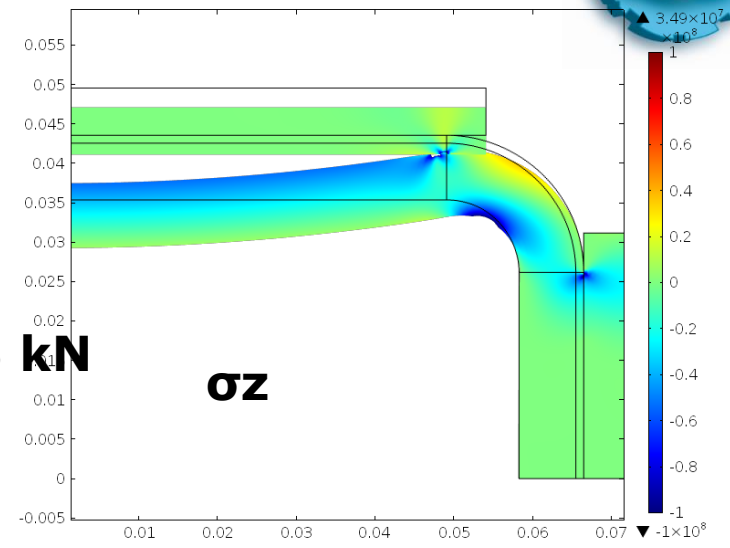
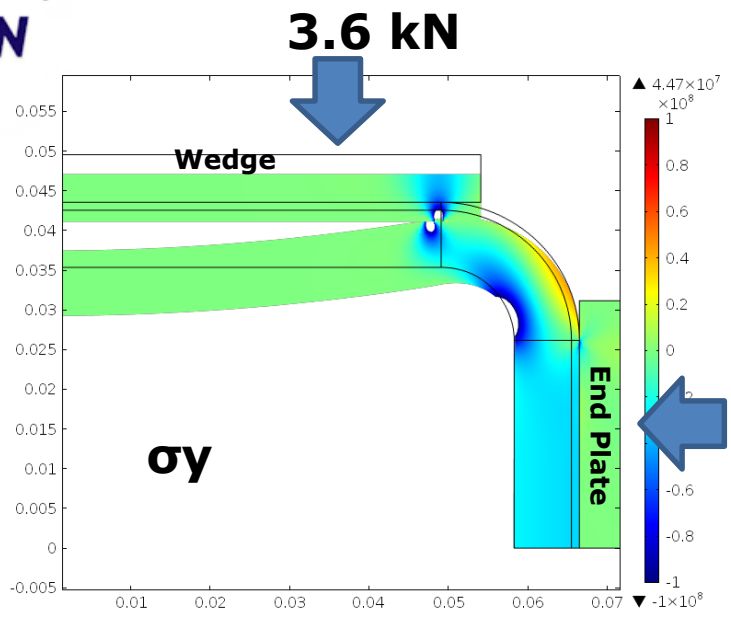
Impregnated coils are markedly anisotropic and strongly dependant on the components mixture. A summary of literature properties has been done, but the value chosen (68 GPa) is found from volumes' rule.

Planned (before magnet construction)

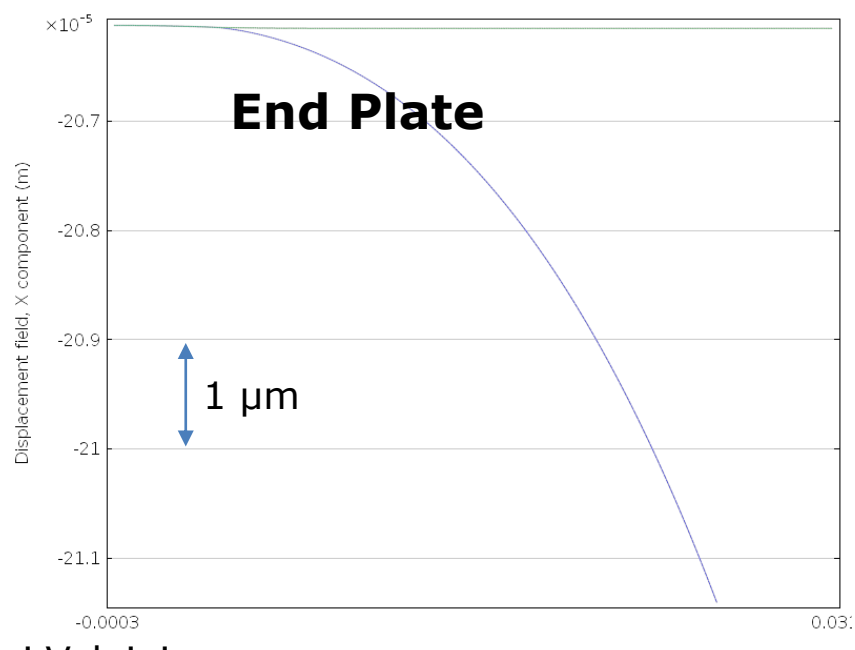
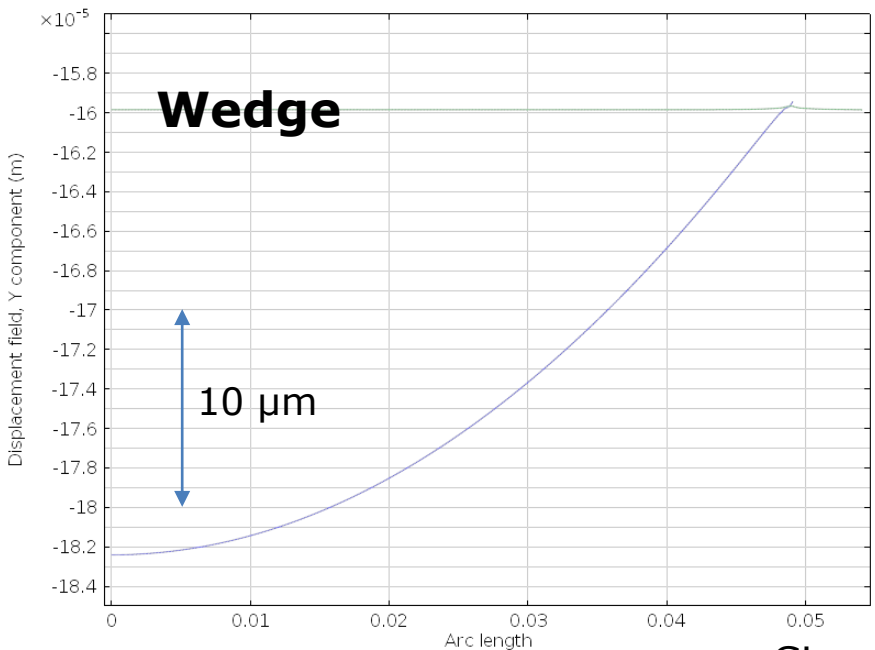
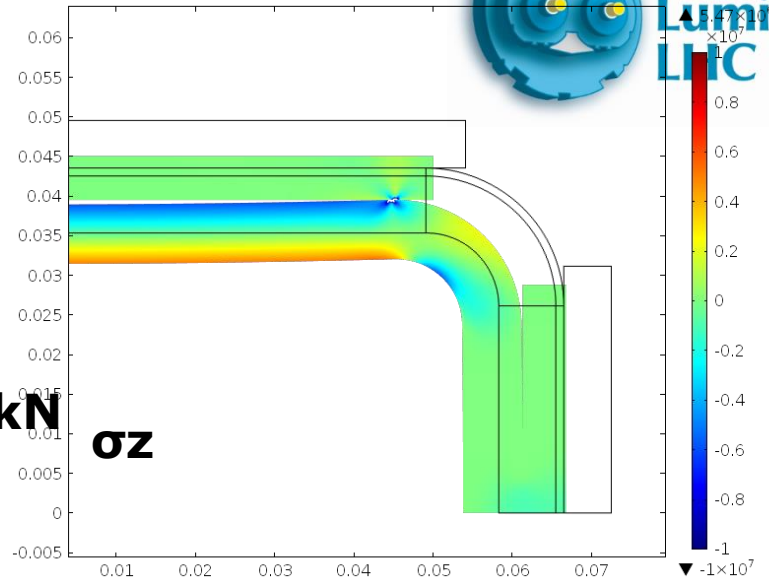
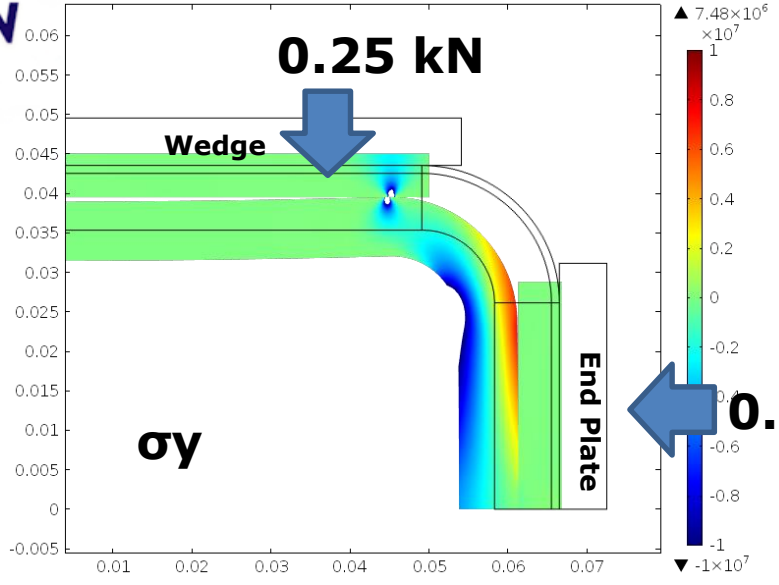
to measure overall deformation of TC04 as a function of applied stress on short and long sides;

to perform Young's modulus measurements on samples from a coil;
thermal contraction

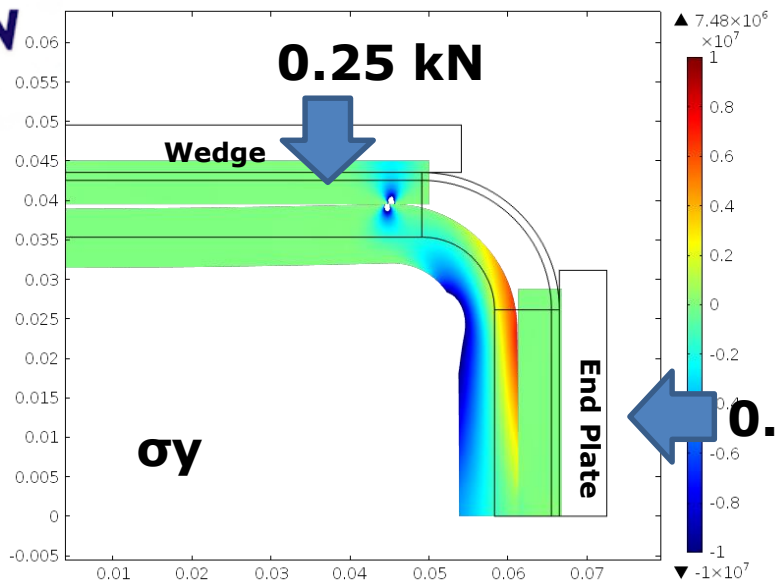
Coil deformation @ RT



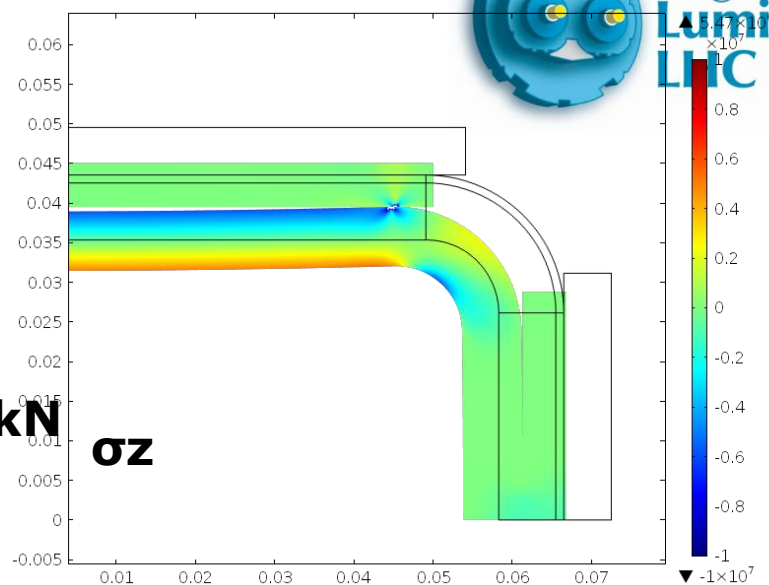
Coil deformation @ 4K



Coil deformation @ 4K w/I

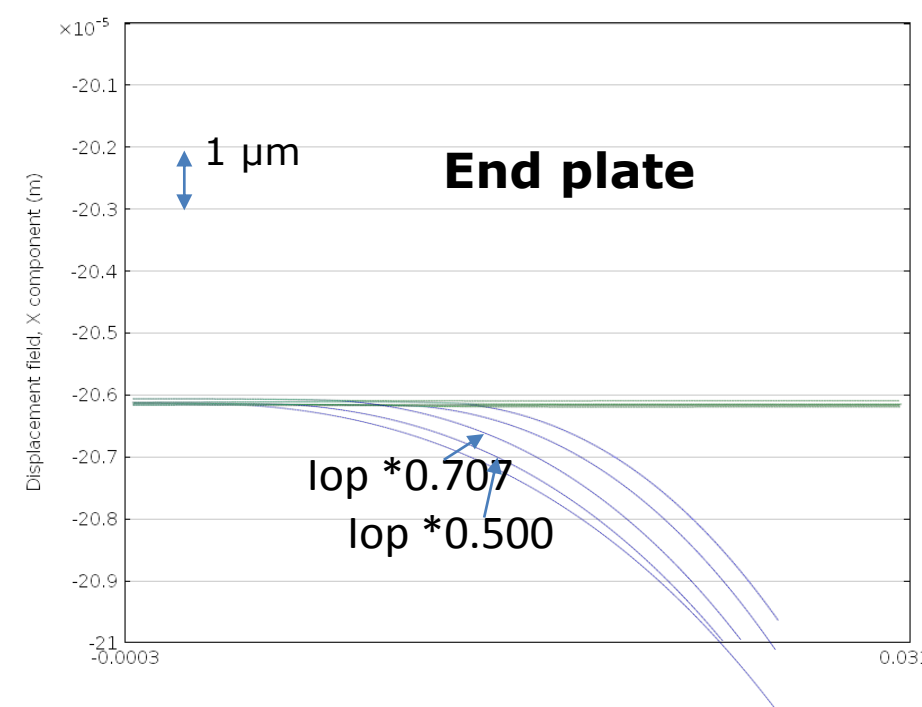
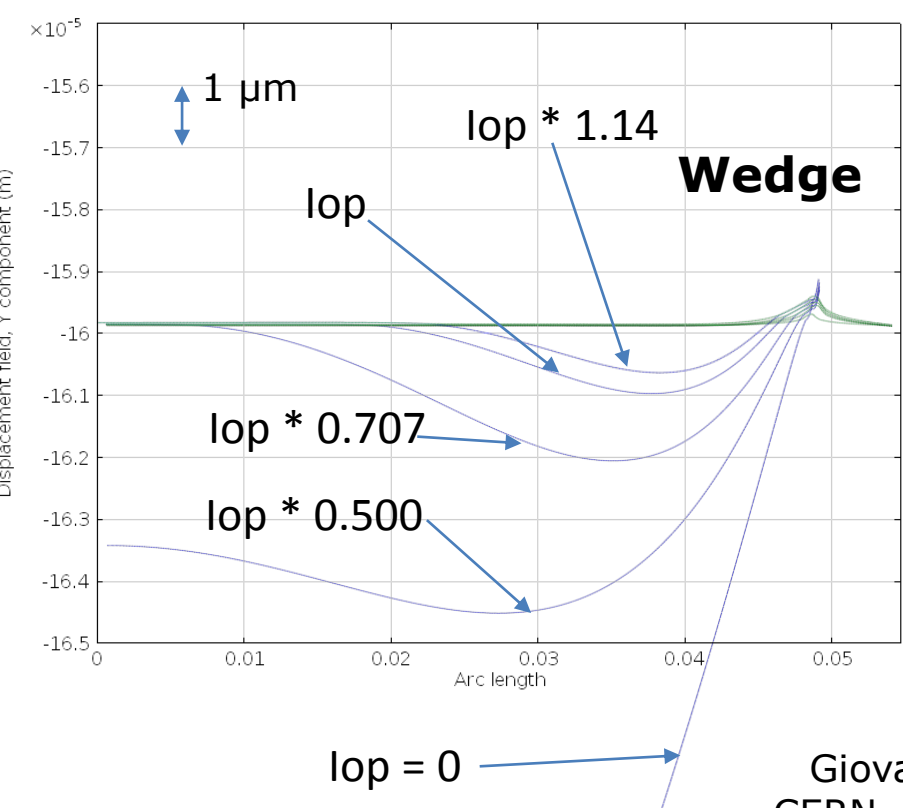
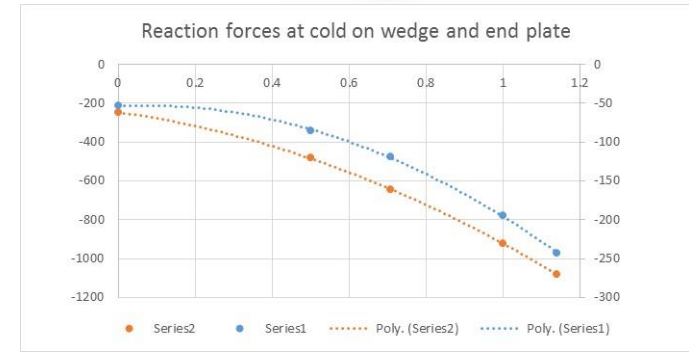


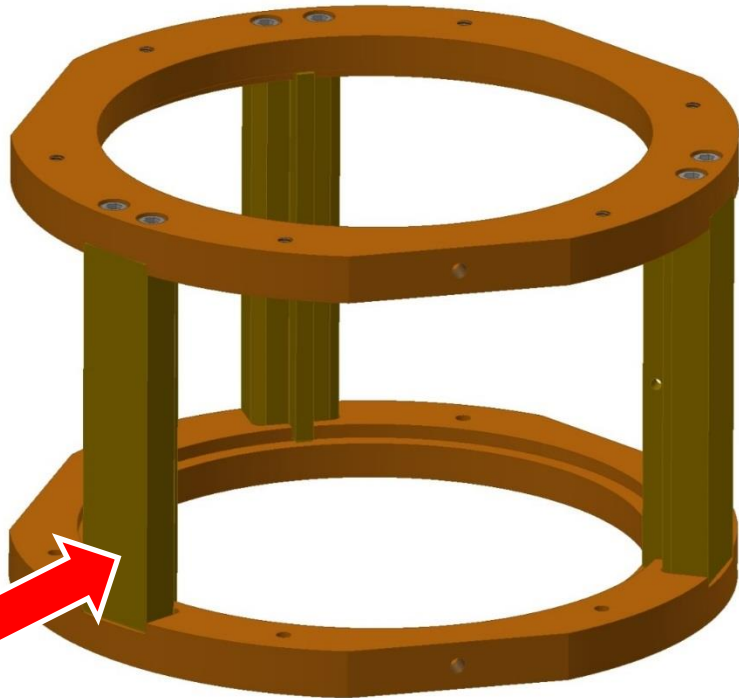
0.06 kN



Coil deformation @ 4K w/ Iop

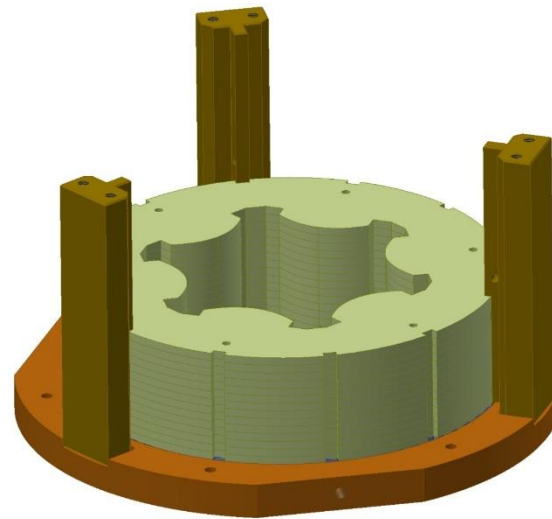
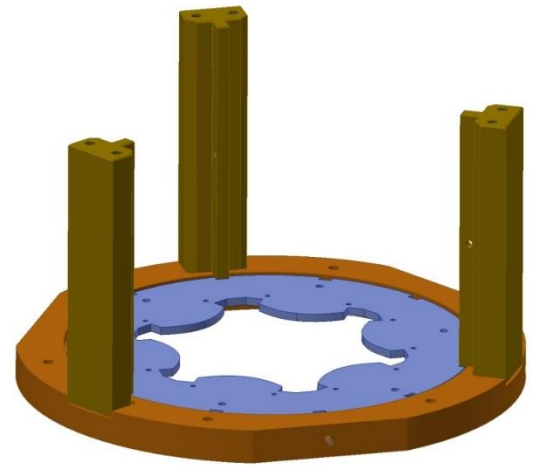
Case	Reac. on wedge	Reac. on end plate
	N	N
RT	-3,600	-3,000
4K, I=0	-250	-60
4K, I=Iop * 0.5	-470	-85
4K, I=Iop * 0.707	-630	-120
4K, I=Iop	-910	-200
4K, I=Iop * 1.14	-1,100	-250



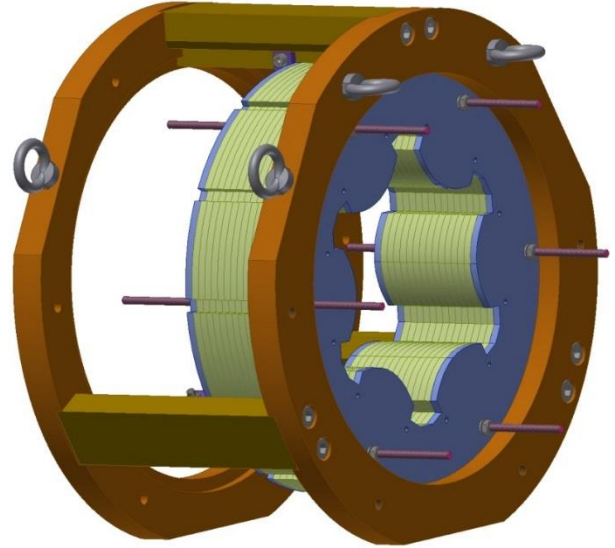
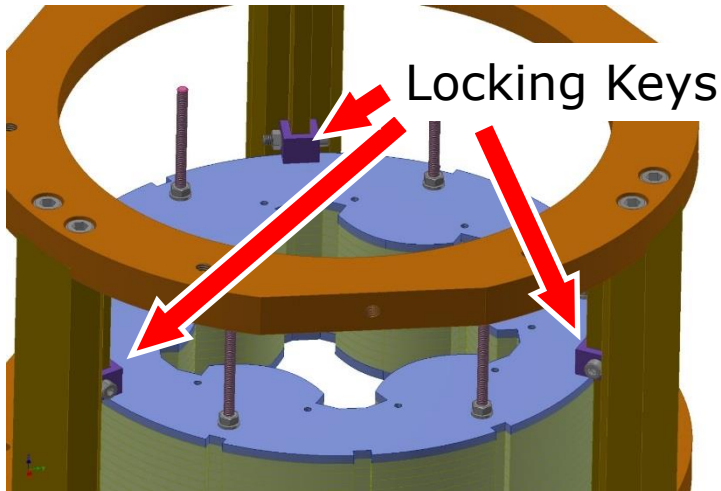
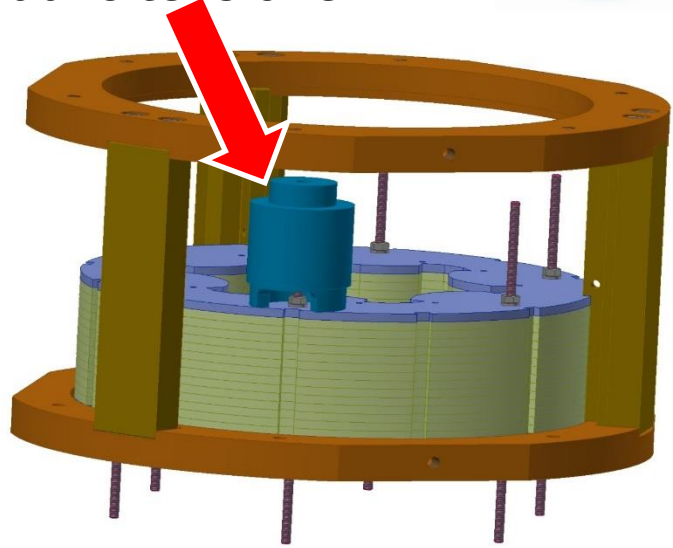
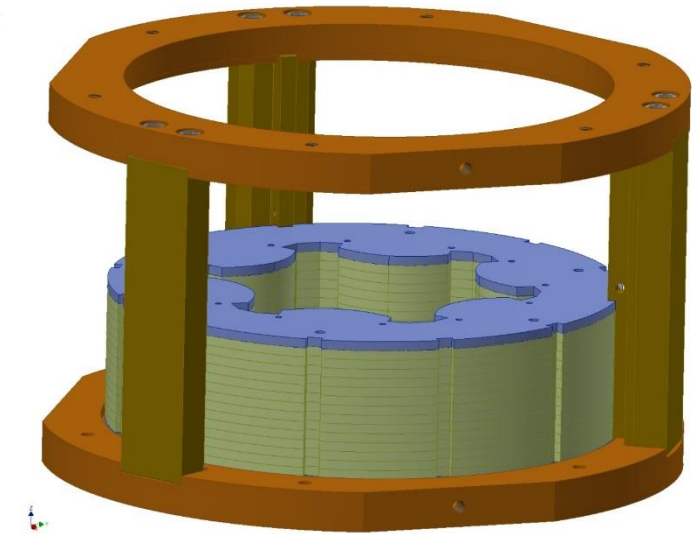


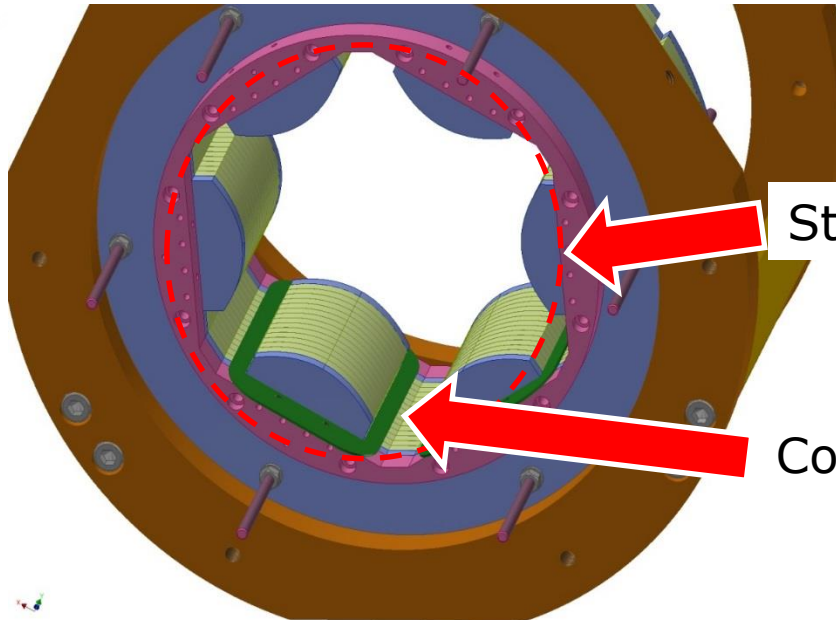
Alignment rail

Assembly tool



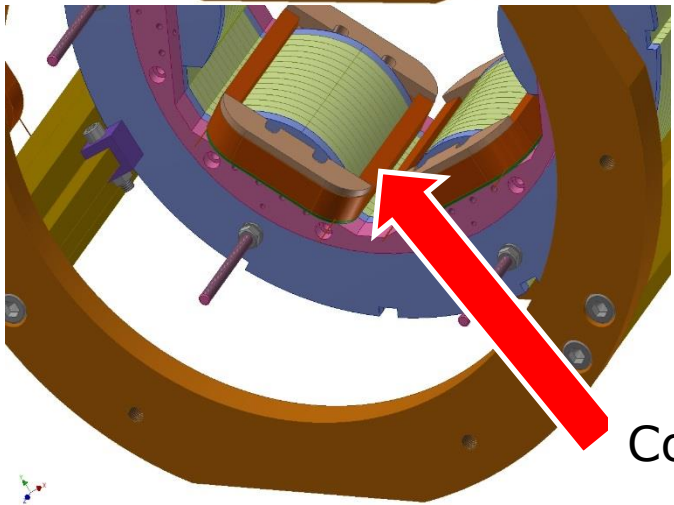
Hydraulic tensioner



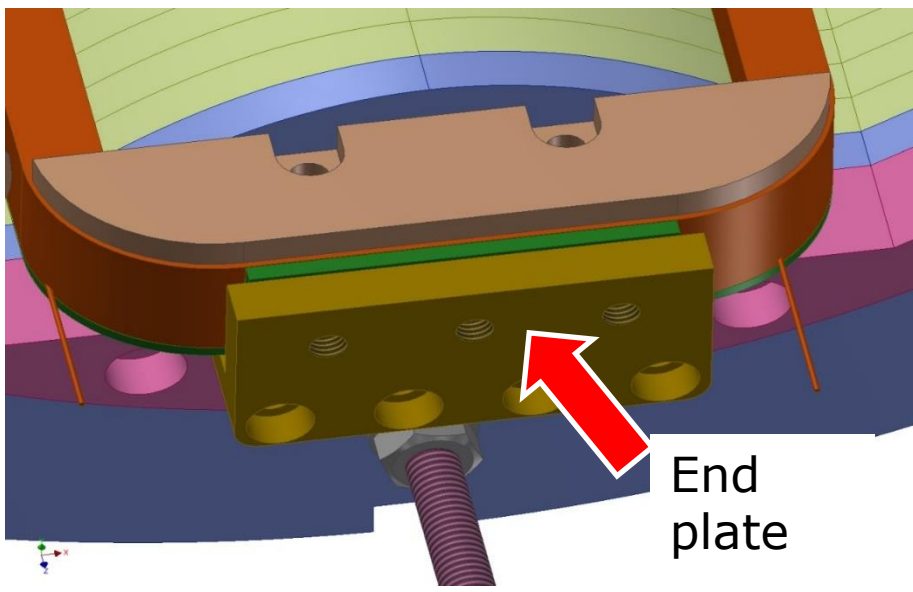


Stainless steel ring

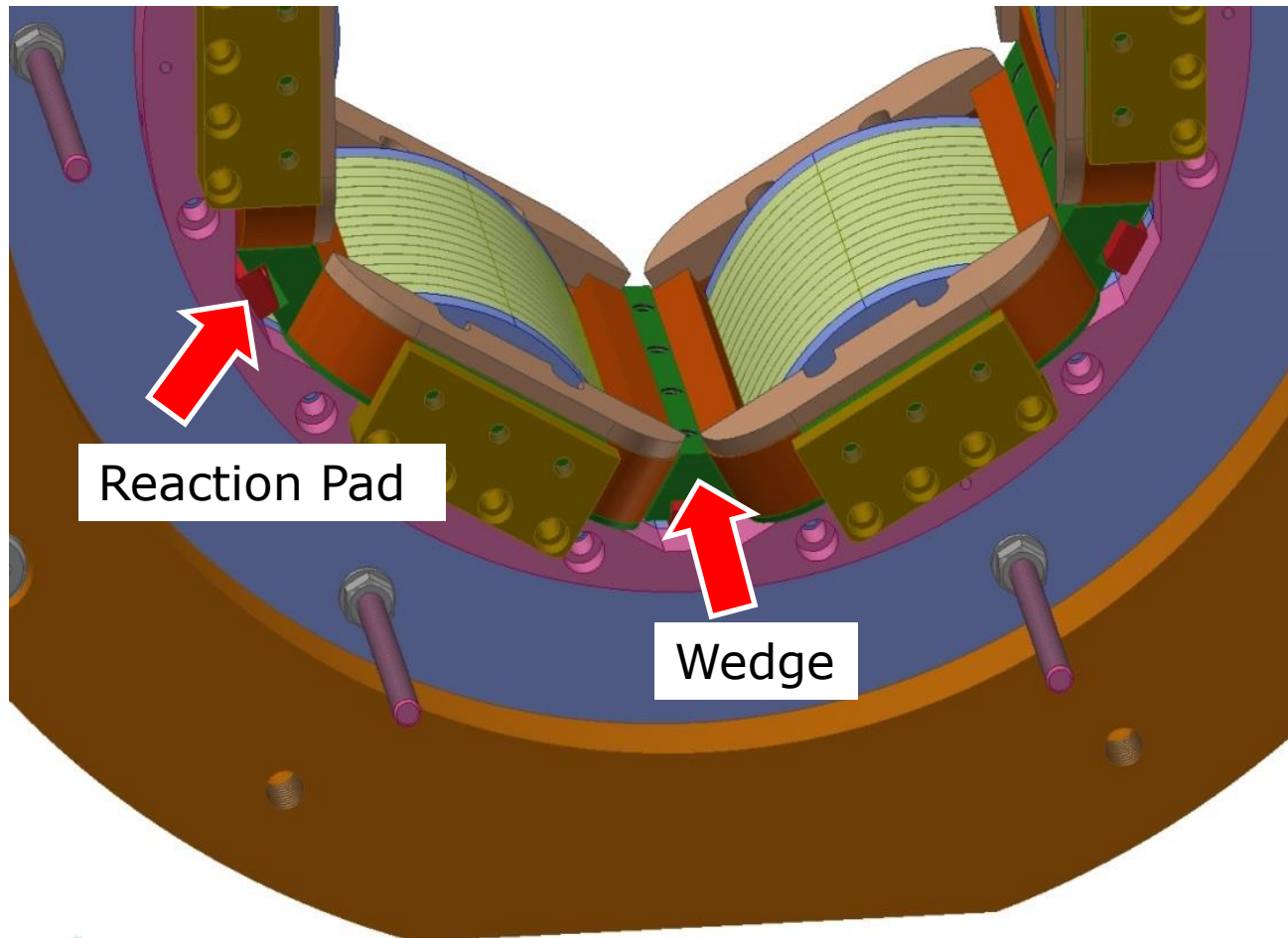
Coil spacer



Coil



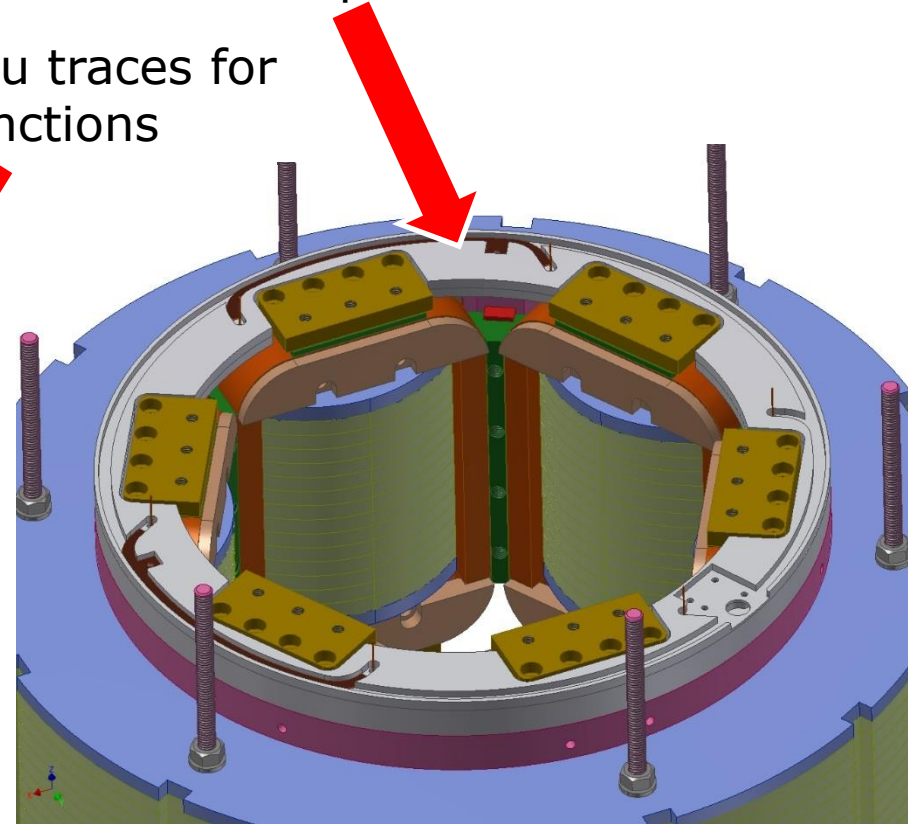
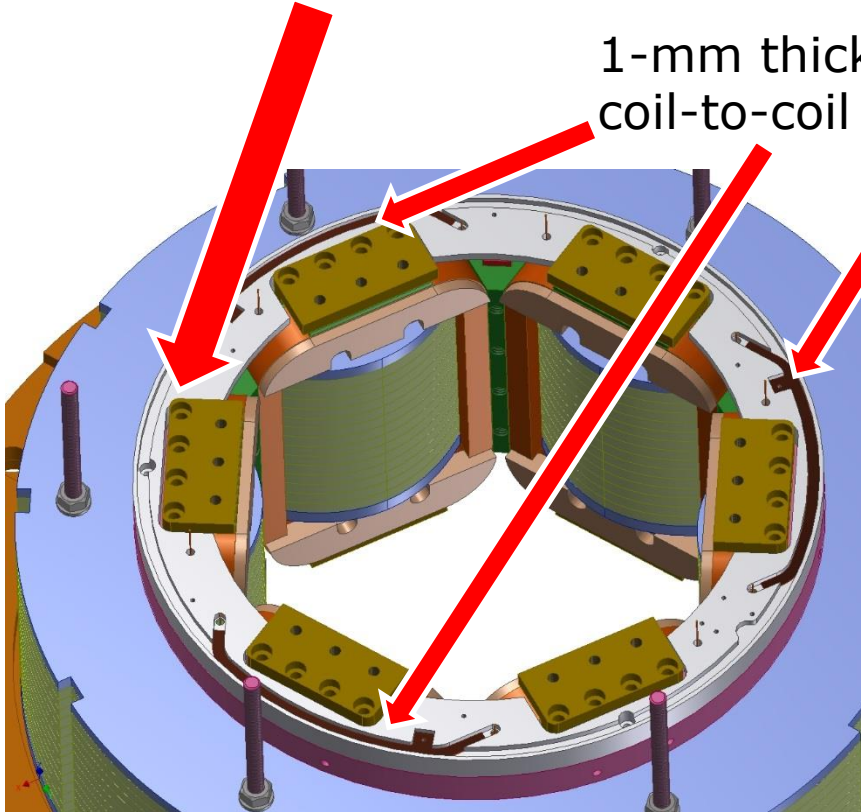
End plate



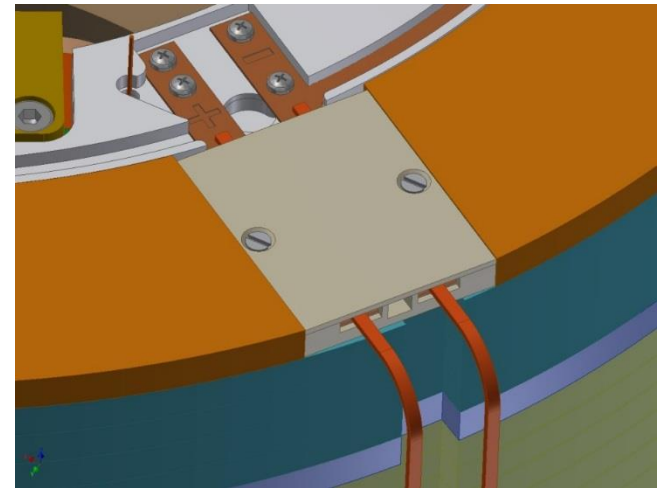
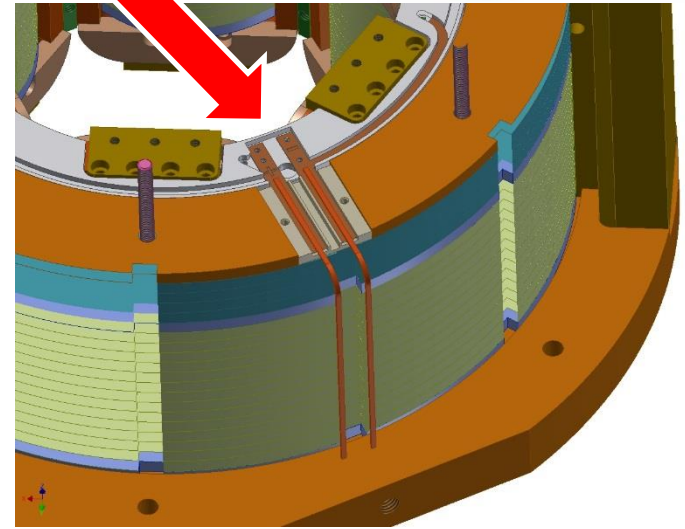
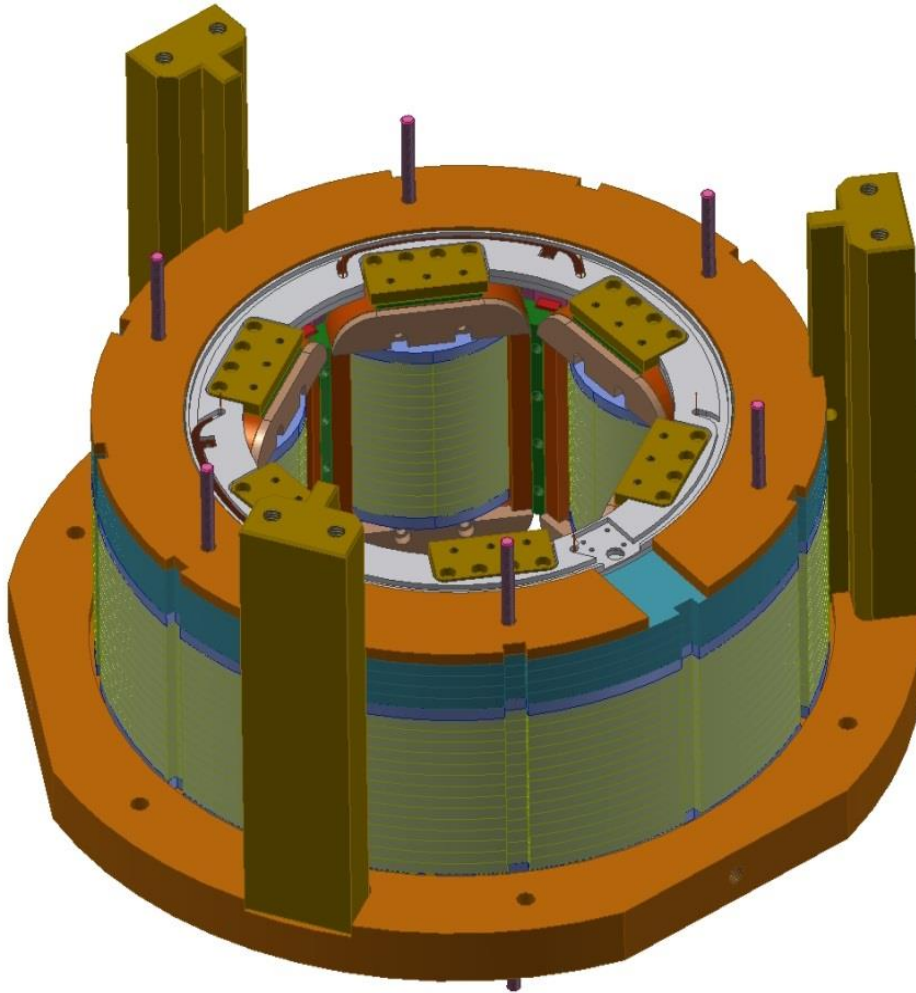
Duratron plate #1

Duratron plate #2

1-mm thick Cu traces for coil-to-coil junctions

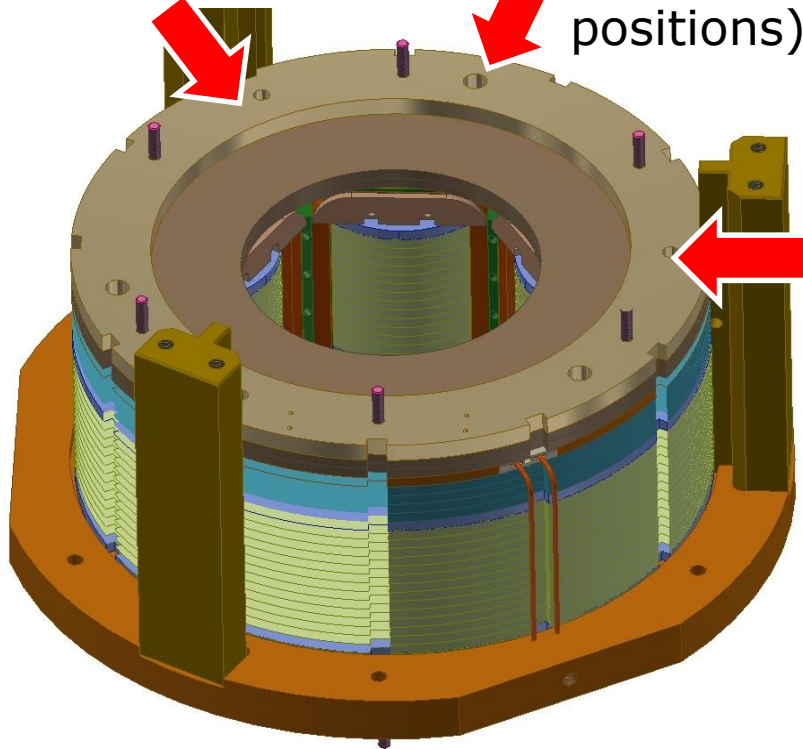


Current connection

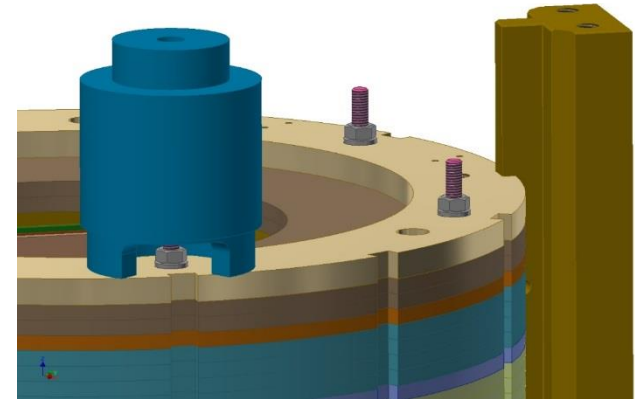


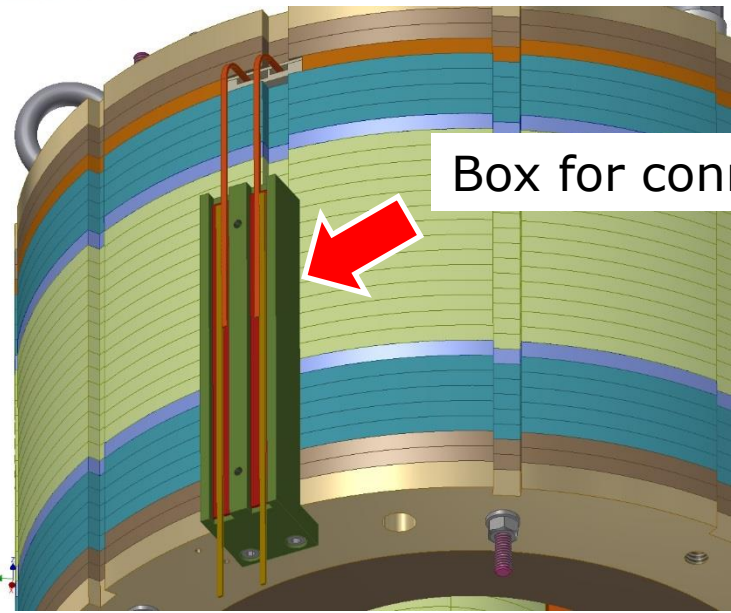
Stainless steel end ring

3 x D12 H7 hole for CCR (preliminary positions)



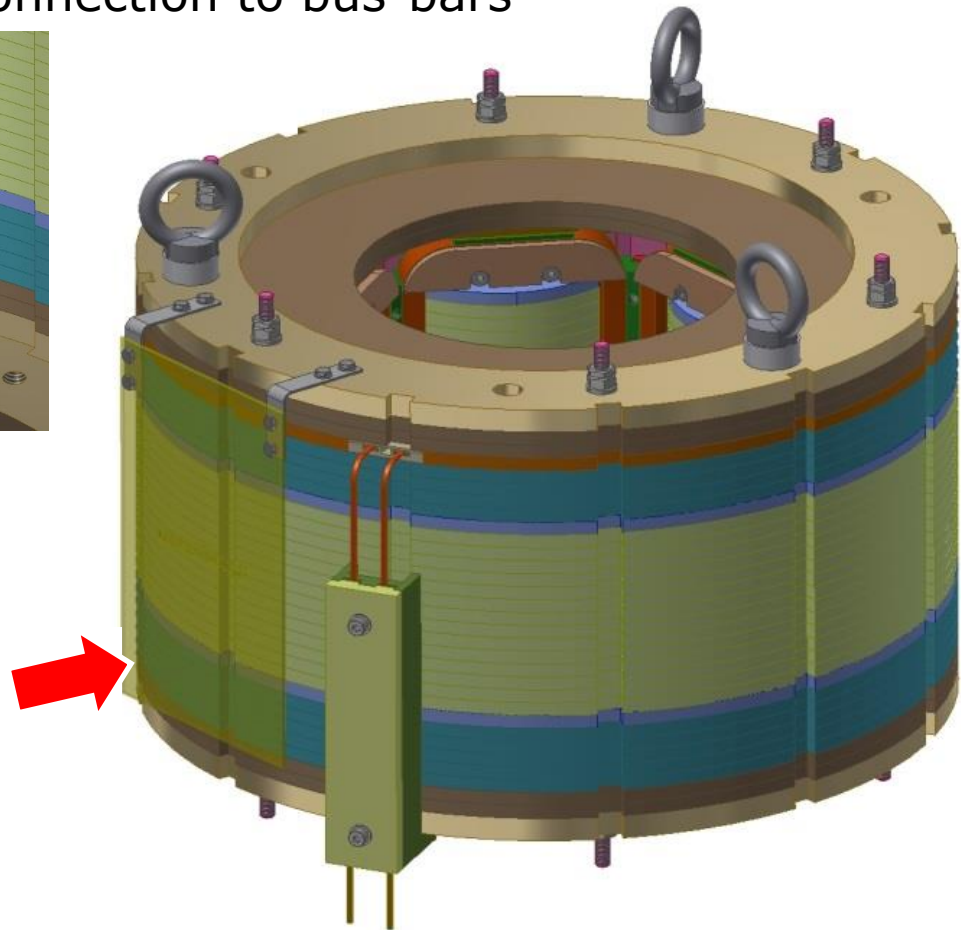
3 x M10 hole for longitudinal connections (preliminary positions)





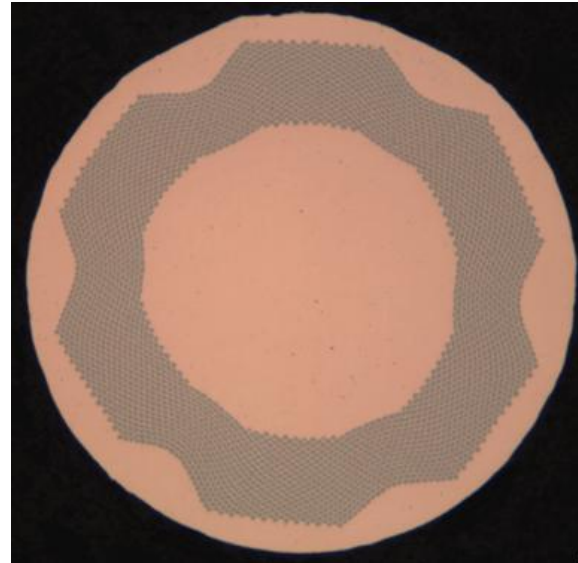
Box for connection to bus-bars

Voltage signal board with current-limiting resistances



4. Superconductor & Coil Manufacture

- *Small wire (low operating current), but not too small (must be easy to handle, insulation should not reduce too much the J_e)*
- *High Cu content (again, low operating current, 4-pole protection)*
- *Off the shelf product: small amount required (10's of kg)*
- *Small filament: not a strict requirement, but these magnets are designed to operate in the whole range $0-I_{max}$*



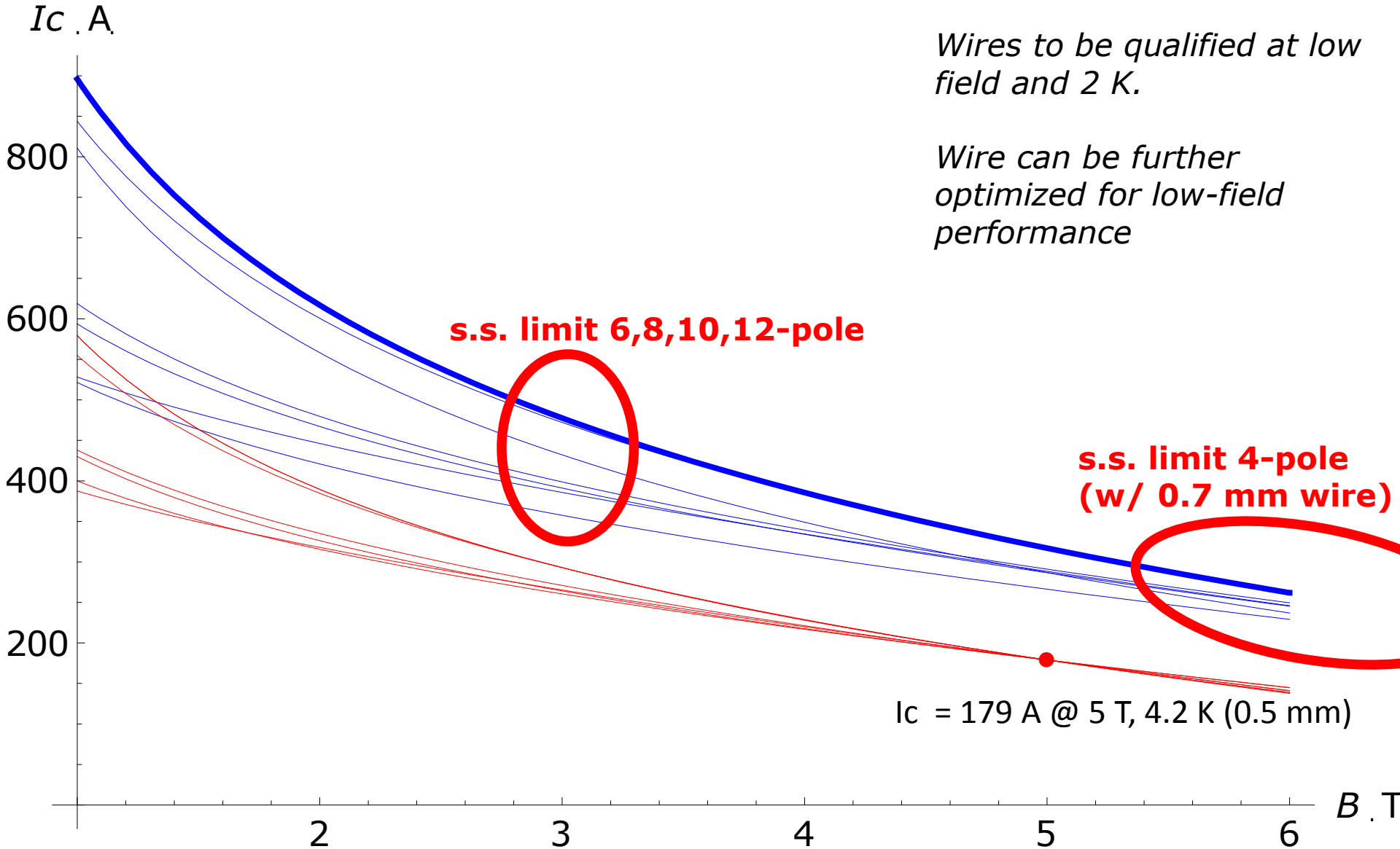
*SC wire procured
35 kg*

*SC wire required for series
~ 150 kg*

Bruker-EAS
NbTi for Fusion application
Fine filaments ITER PF wire
Wire type 2
 Cu:NbTi \approx 2.30
 Number of filaments 3282
 Wire (filament diameter)
 0.5 mm (5.5 μ m)
 0.7 mm (8 μ m)
 S2-glass insulation,
8 km + 8 km

Caveat artifex:

I_c low field extrapolation could be somewhat inaccurate



Wires to be qualified at low field and 2 K.

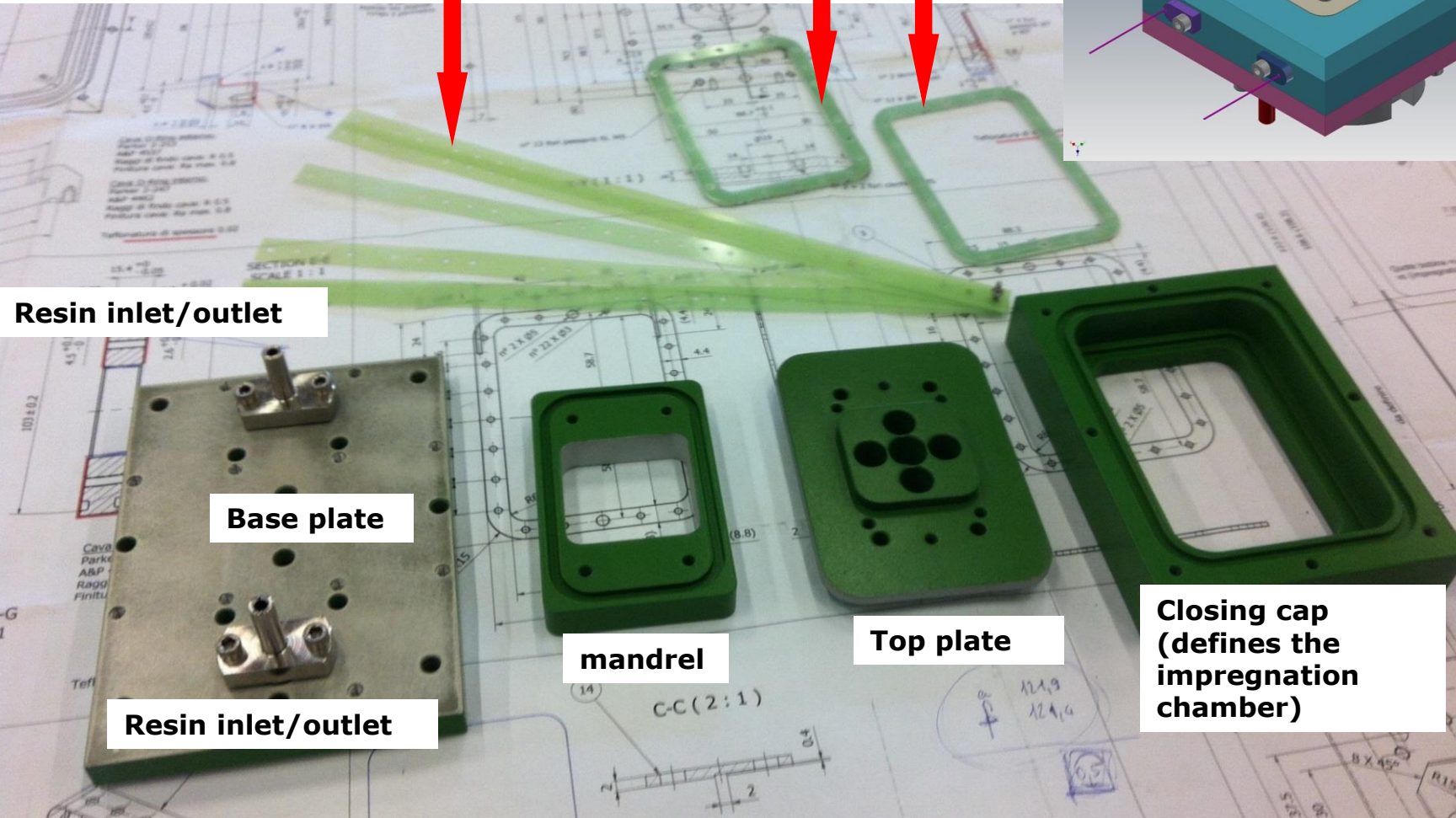
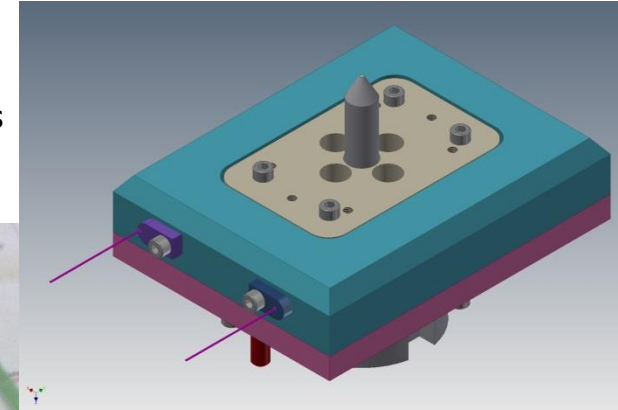
Wire can be further optimized for low-field performance

Coil winding & impregnation tooling

Insulation scheme:

- wire w/ S2 glass 0.14 mm thick (on dia)
- ground insulation:

G11, 2 mm thick plates on both sides of the coil, including the wire exits
 G11 thin, flexible layer on the inner wall of the coil;
 S2 tape on the outer wall



Resin inlet/outlet

Base plate

mandrel

Top plate

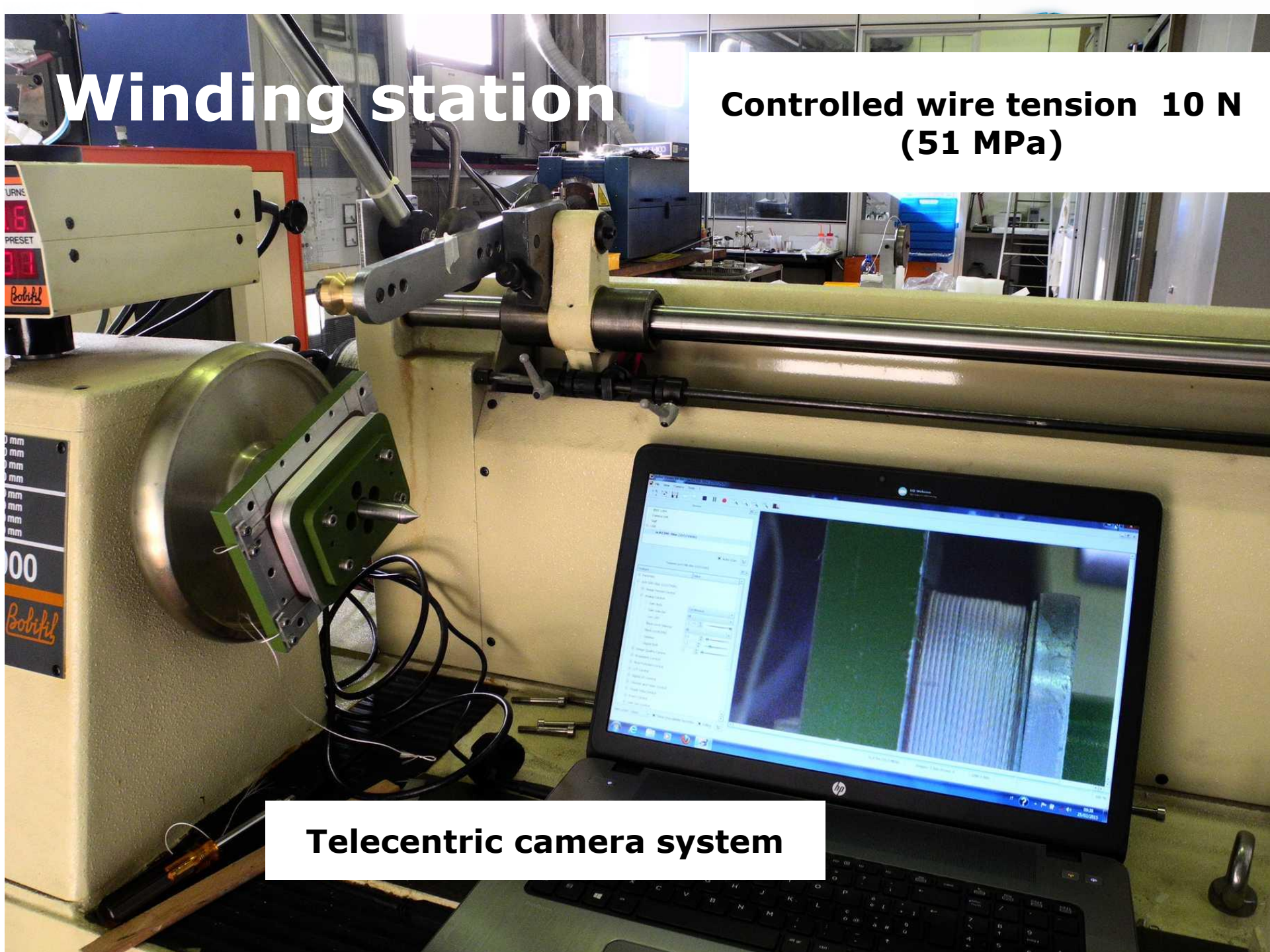
Closing cap
 (defines the
 impregnation
 chamber)

Resin inlet/outlet

Winding station

Controlled wire tension 10 N
(51 MPa)

Telecentric camera system



Winding quality

A close-up photograph of a metal coil winding on a machine. The coil is made of many thin, parallel metal strips. Two red ovals highlight specific areas of the winding. The top oval highlights a section where the strips are slightly separated, creating a small gap. The bottom oval highlights another section where the strips are more closely packed. The background is blurred, showing parts of the machine and a blue wall.

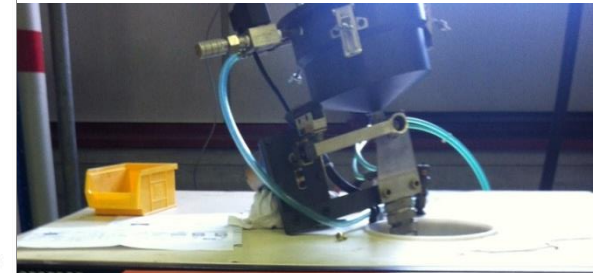
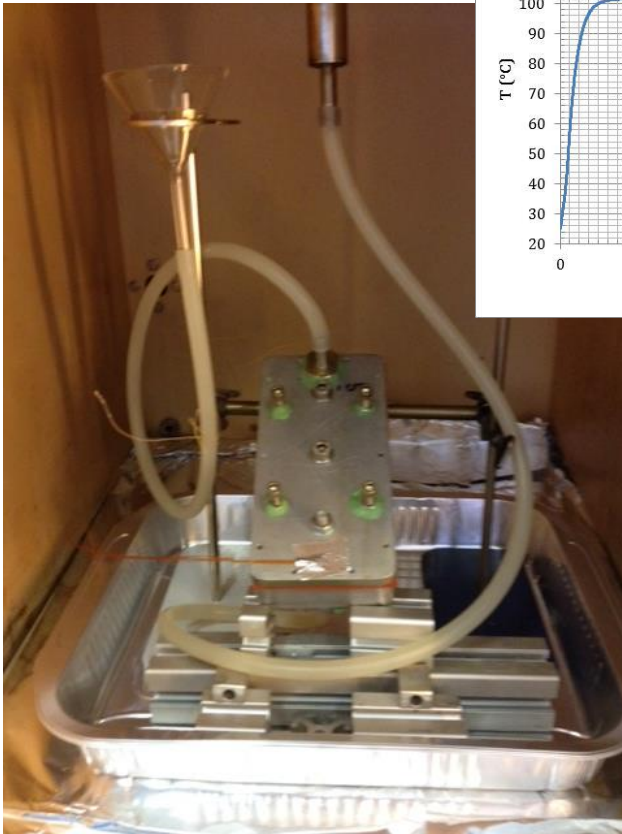
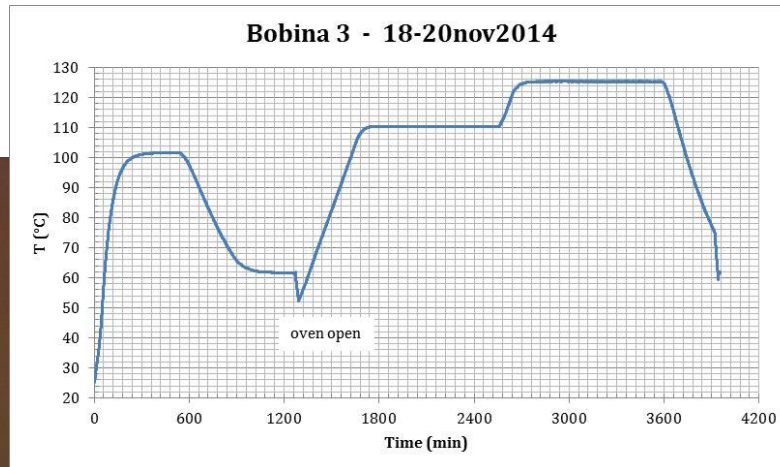
See following slides

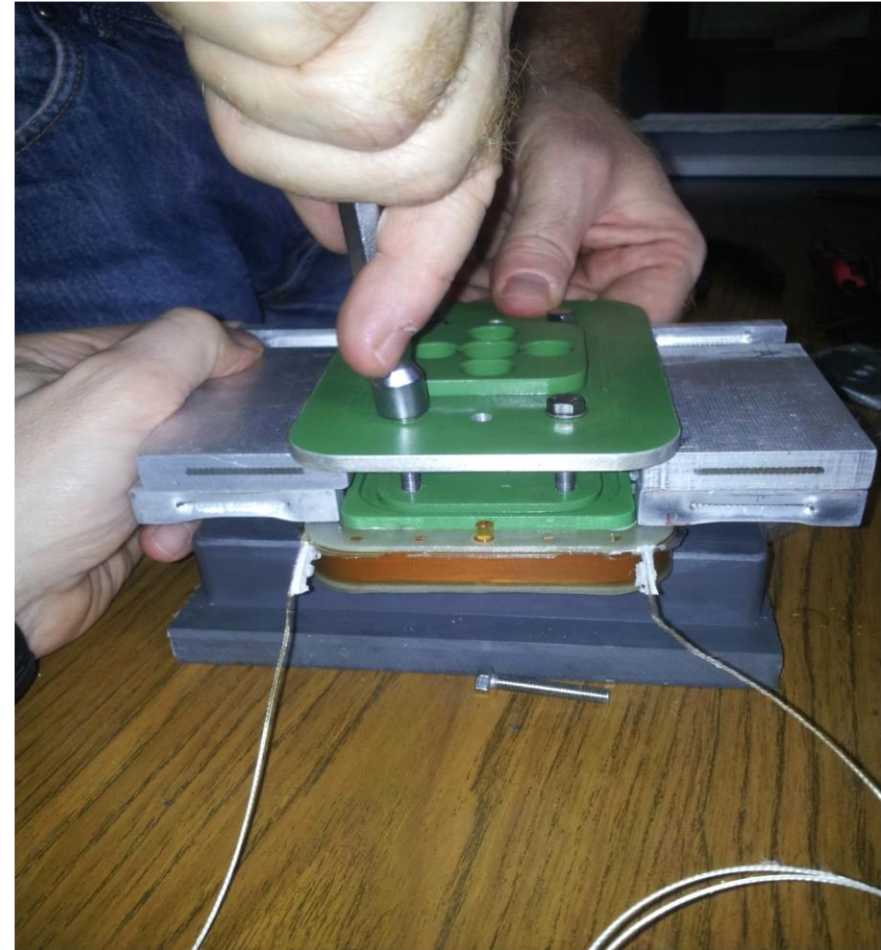
A small gap between turns appears sometimes. The filling factor can not be close to 100%, to allow proper alignment of the turns.

Oven & impregnation

CTD-101K resin

Temperature monitored with a PT100 on the mould, in agreement within $\pm 1^\circ\text{C}$ wrt the set temperature (in stationary conditions)



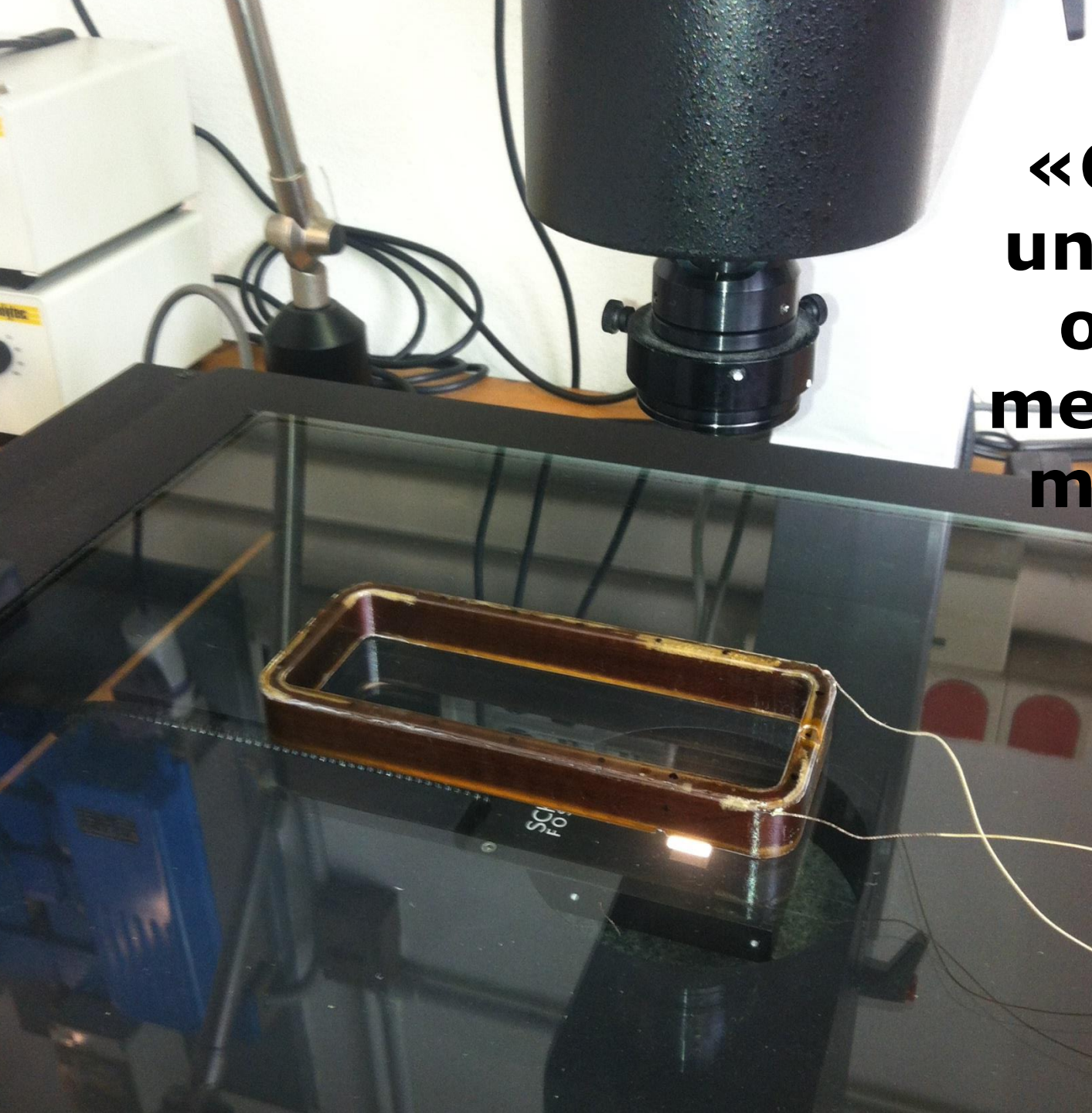


A number of tests is performed on the coil during the manufacture steps. These are collected into a single document, which is meant to evolve into a formal Quality Control Plan, with well defined steps, goals and procedures.

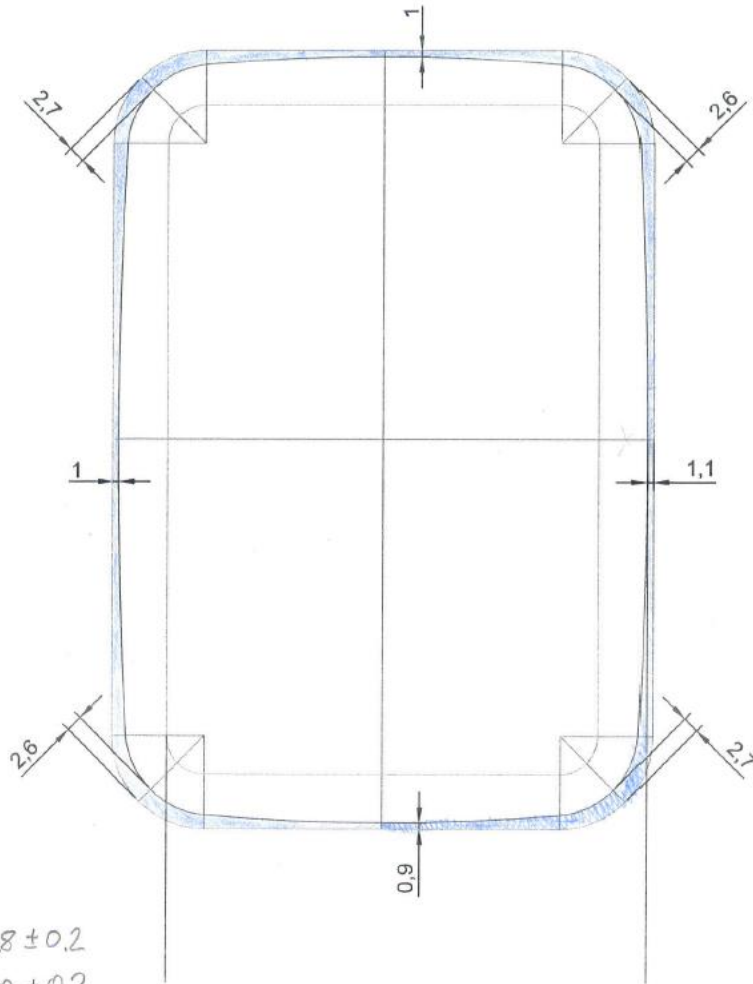
Test protocol

- Coil resistance @ RT , typical values 9.2 ± 0.001 ohm, coil temperature measured with 0.1 °C accuracy
- Ground insulation test @ 5 kV > 200 GΩ
- Dimensional measurements w/ gauge & optical measuring apparatus
- Thermal shock @ LN on coil and on resin sample
- Resistance & ground insulation test repeated after thermal shock
- Inductance measurement

**«Coil 1»
under the
optical
measuring
machine**



TC4
quote rilevate il 13gen2015



28 ± 0.2

10 ± 0.2

$\Delta 1.8 \pm 0.3$

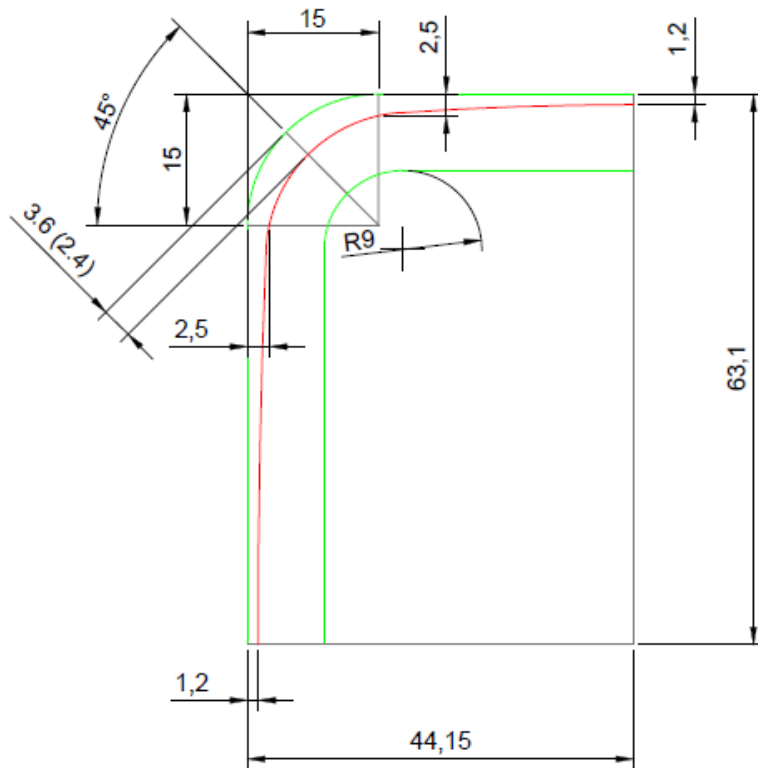
Measurements performed on the coil after winding shows an ovalized shape, with a difference in thickness between corners and straight section of 1.8 mm.

To avoid resin-rich zones in the corners, ad-hoc fillers made with G10 strips and S2 fiberglass were added to the corners. This technique is not suitable for series production, and must be improved.

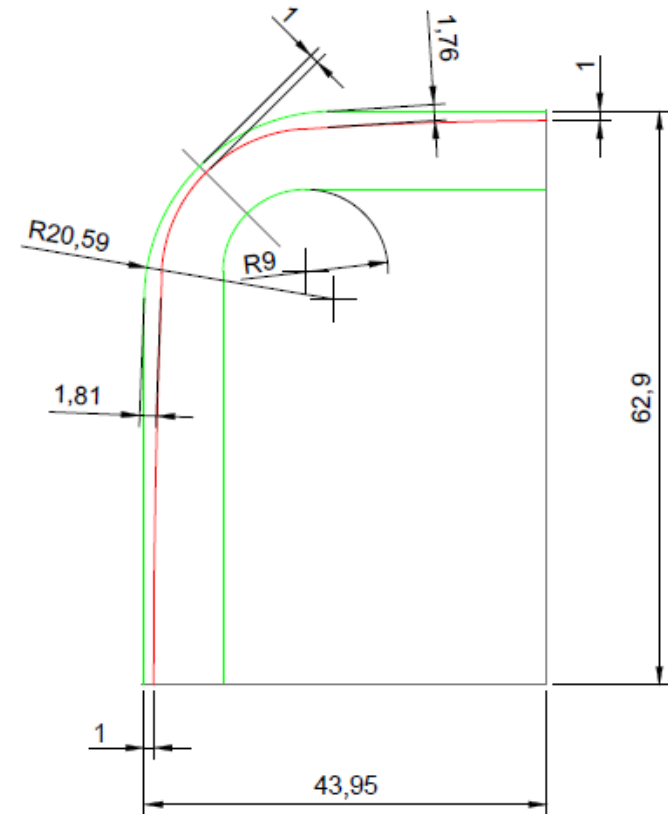
This coil (#4) has nonetheless been successfully impregnated and has been tested at LHe.

avvolgimento del 24feb2015
distanze medie

nuovo profilo esterno con 1mm di margine



results of the improved winding procedure (measured values)



New shape of the impregnation mould outer part

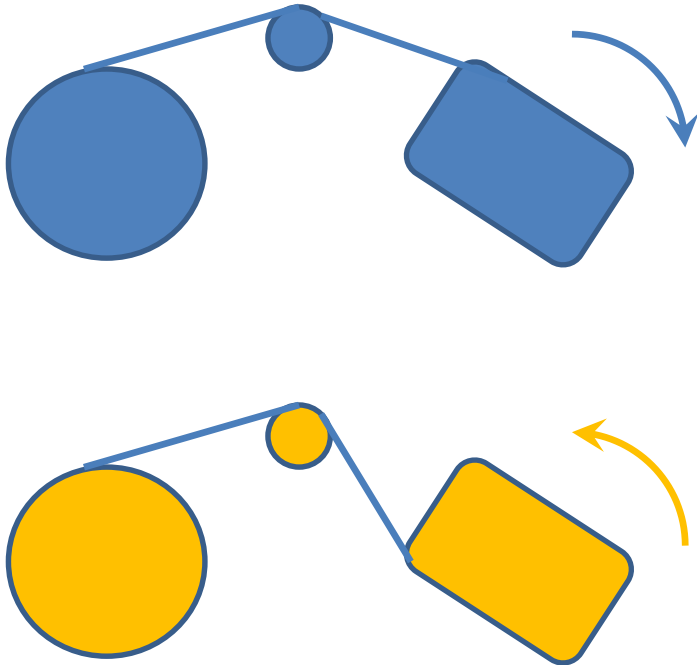
Making it square

modifying the SC wire circuit

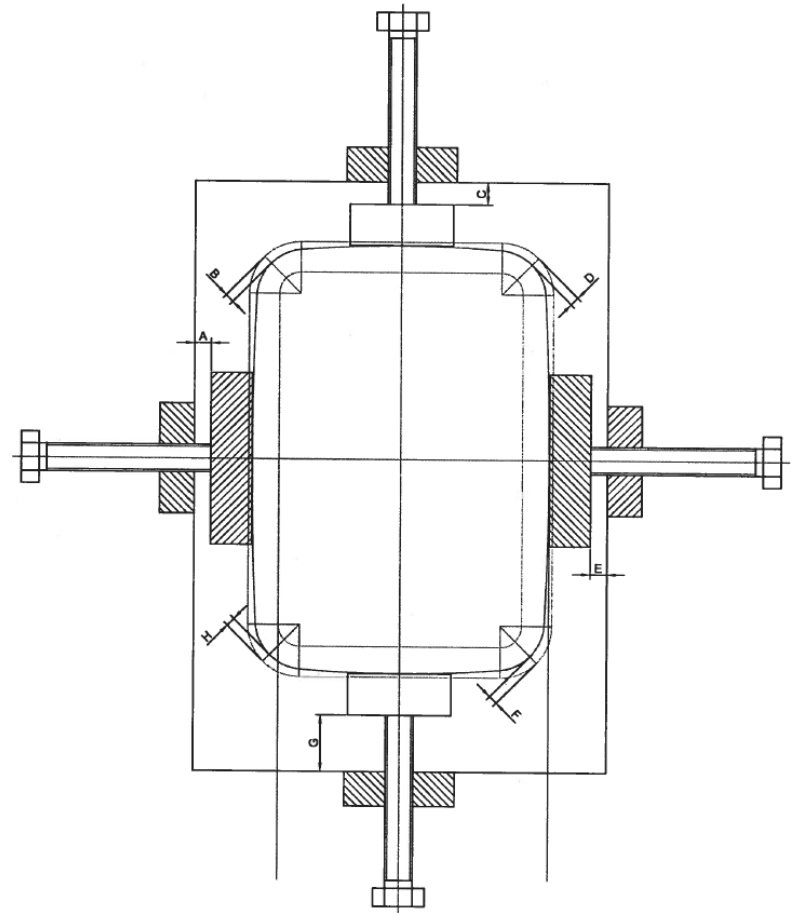
pulley

winding tool

pay-off spool



applying pressure

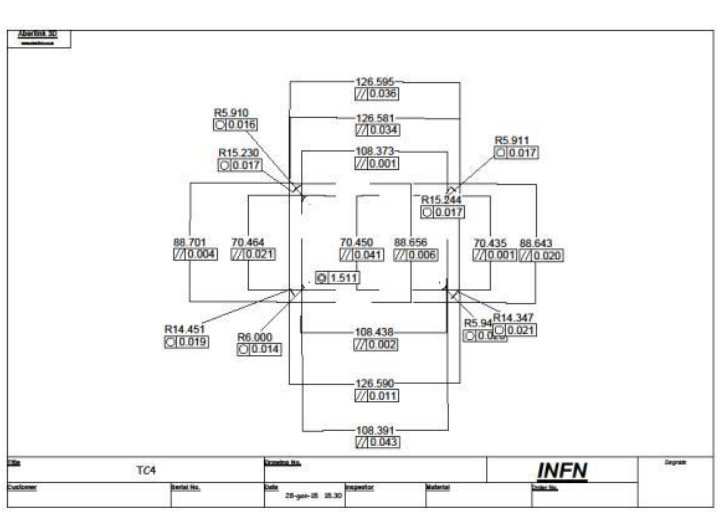


Coil #3

Inner Width	Outer Width	Inner Length	Outer Length
70.164	88.725	108.189	126.621
70.198	88.772	108.201	126.576
70.145			
70.169	88.749	108.195	126.599
0.027	0.033	0.008	0.032

Coil #4

Inner Width	Outer Width	Inner Length	Outer Length
70.464	88.701	108.373	126.595
70.45	88.656	108.438	126.581
70.435	88.643	108.391	126.59
70.450	88.667	108.401	126.589
0.015	0.030	0.034	0.007

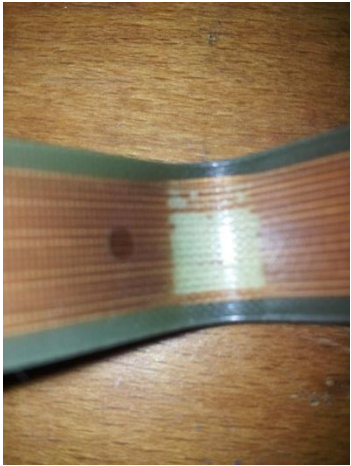


Measurements done after extraction and repeated after some days to detect any «creep». No evidence found

Inner Width	Outer Width	Inner Length	Outer Length
70.424	88.718	108.349	126.571
70.414	88.671	108.364	126.576
70.402	88.654	108.411	126.595
70.413	88.681	108.375	126.581
0.011	0.033	0.032	0.013

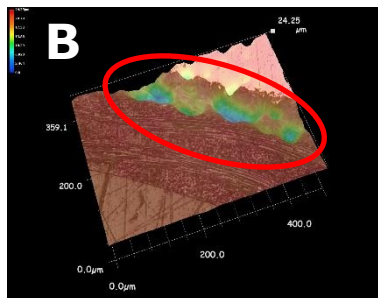
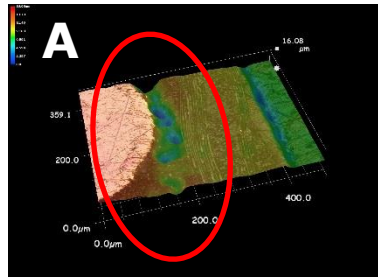
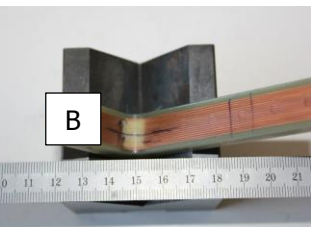
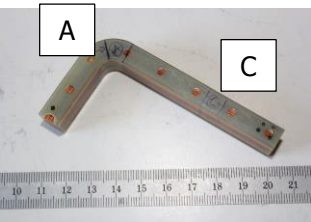
Differences between #3 and #4

Inner Width	Outer Width	Inner Length	Outer Length
0.263	-0.075	0.193	-0.014
0.032	0.056	0.047	0.035

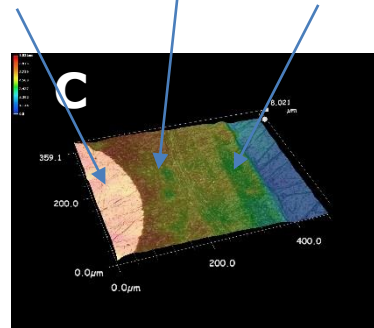


This nasty feature has appeared in the four inner corners, essentially to the same extent. Most surprising, it has not shown up immediately, but after a few days, in a progressive fashion. An attempt to apply penetrating liquids on a polished cross section has not provided any sign of cracks.

Alexandre Geradin, TE-MME-MM, has performed an investigation with optical microscopy, and he was able (EDMS report 1497272) to identify voids in the insulation area of the wires in the corners, but not in the straight section.



wire insulation G10



The conclusion is that a delamination, or a failure of impregnation, took place in the wire insulation, not in the 0.2 mm thick G10 layer.

A possible explanation could be that this coil was wound with a wire having starch (instead of silane) sizing, wrongly supplied by B-EAS.

Indeed, no such problem has appeared in the following coil, wound with silane-S2 insulated wire.



Coil manufacture



Based on the good result of the single coil test (sec. 5), the construction of the six "true" coils for the hexapole has been cleared. They will have

- the same manufacture procedure,
- same choice of the ground insulation, namely G-10 shoulders and S2 fiberglass tape layers,

Following modifications have been introduced:

- minor dimensional changes;
- number of turns 214 (TC04 has 204), based on extensive campaign test and spacers optimization;
- corner filling improved by increasing the external curvature radius

Two winding and impregnation tools/moulds have been machined at an external workshop, and are now Teflon-coated at a specialized company.

G10 is not compatible with the design dose (25 MGy) For next magnets (and in perspective for the sextupole as well), G10 in the coils must be replaced by a suitable material.

Possible choices are:

ULTEM 3D printed items

or

ad hoc S2+CTD101K laminated fiberglass

or

fiberglass loaded ULTEM machined

or

...any other suggestion?

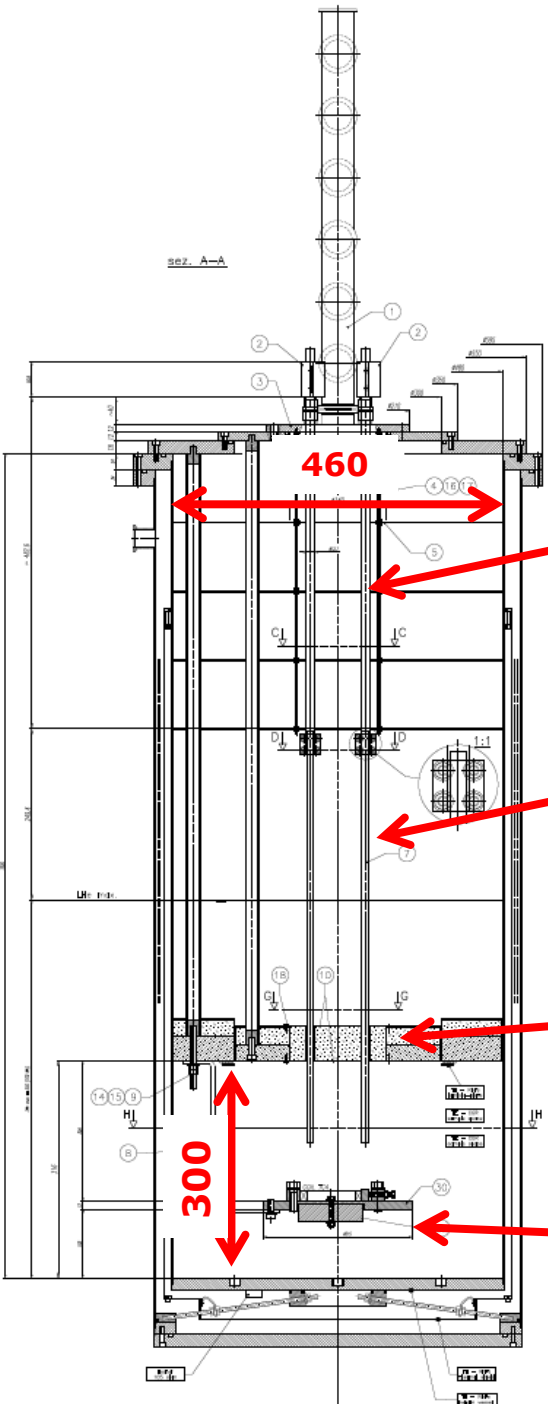


ULTEM items procured, winding & impregnation of a test coil in progress. If successful, may be implemented in a_4/b_4



5. Test @ LASA

Test Station



460

500 A current leads

SC bus-bars
Al-clad NbTi SC
cable for Mu2e TS

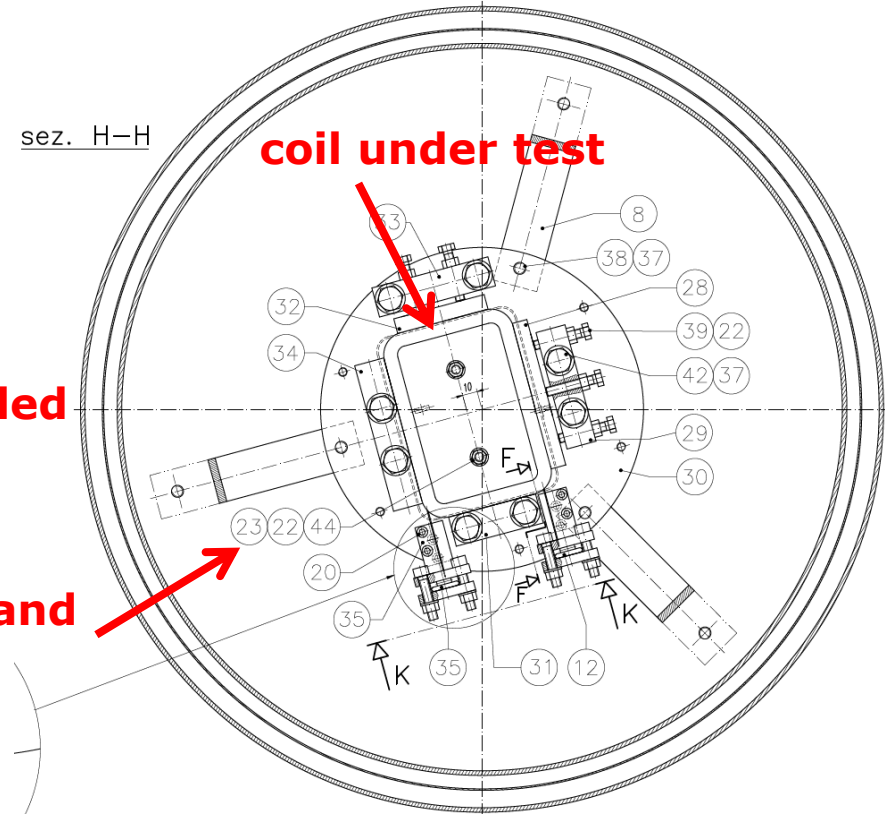
λ -plate for subcooled
operation

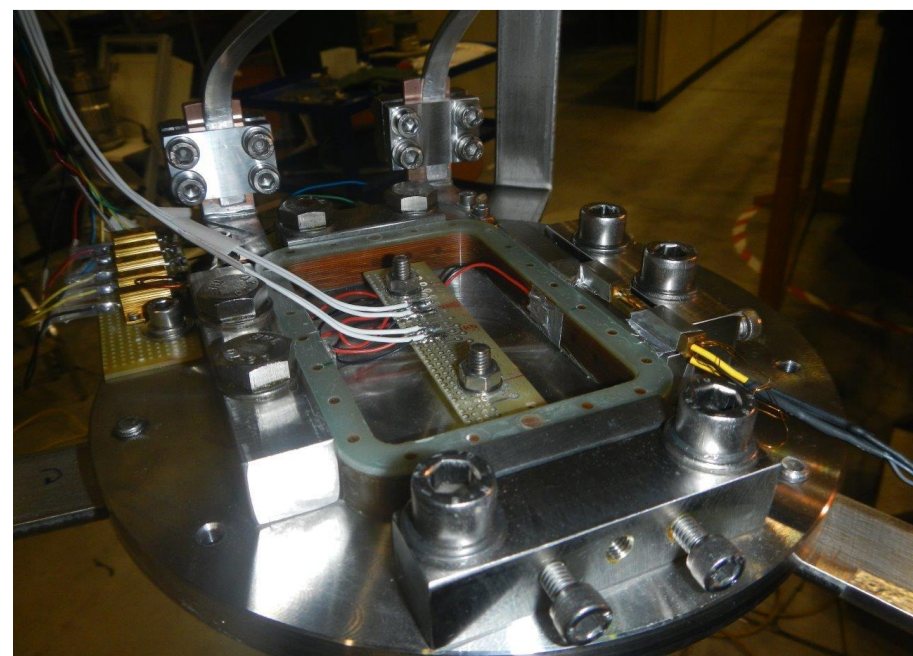
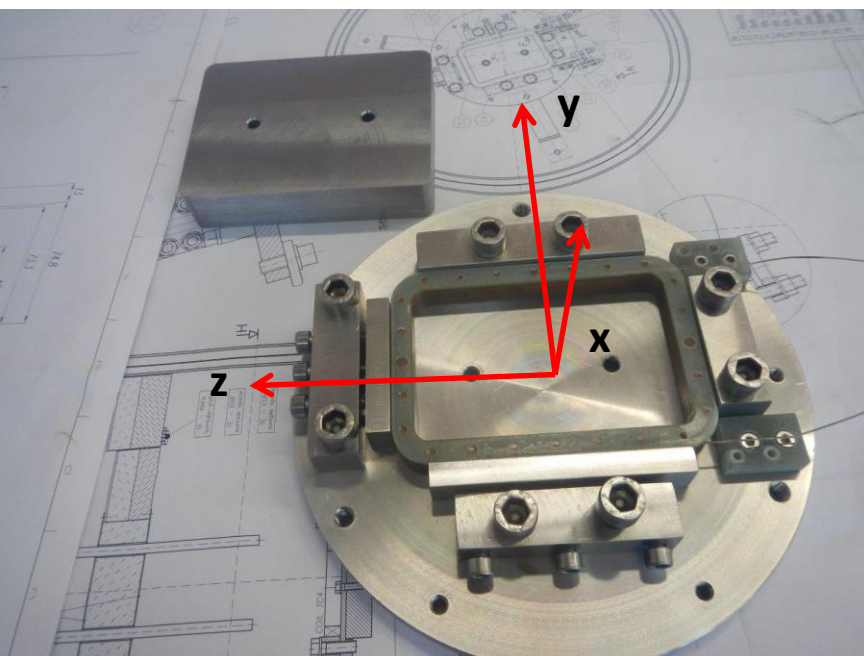
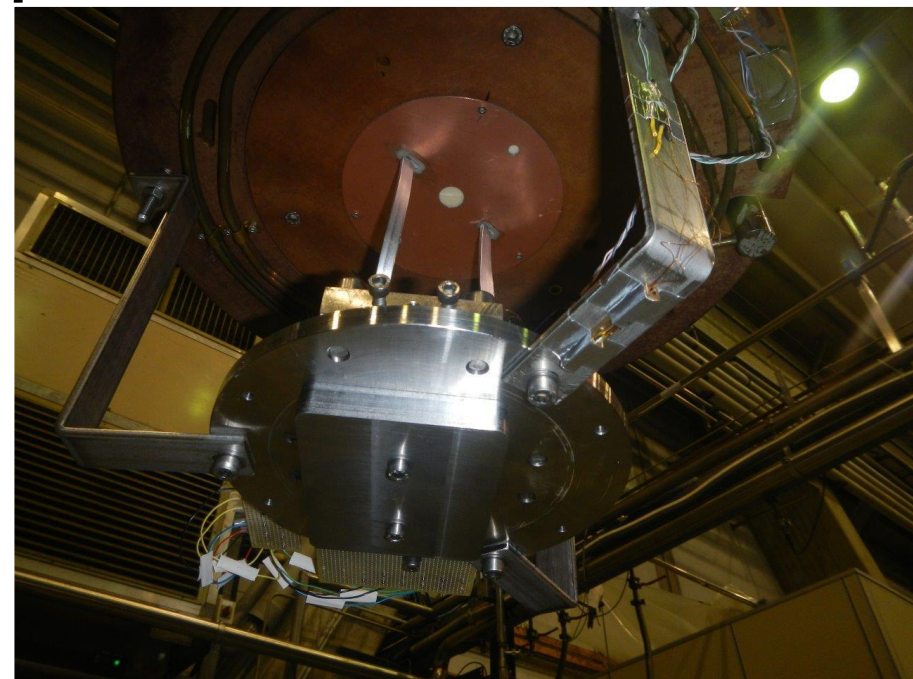
Single coil test stand
(later 6-pole ...)

300

sez. H-H

coil under test







Purpose(s) of the test



- 1) To test a coil in “realistic” conditions to identify major faults in the design/assembly

A magnetic plate creates between iron and the coil an attractive force along the normal of the coil plane. In this way, the e.m. force pattern is more resembling to that experienced by a coil during its operation inside the magnet.

F_x (normal to the coil plane, half coil)	2.9 kN @ lop,	here reached at about 300 A
F_y (normal to long axis, half coil)	1.5 kN @ lop,	“ 250 A
F_z (normal to long axis, half coil)	0.6 kN @ lop,	“ 180 A

Test both at 4.2 K and 2 K

Single Coil short sample limit

295 A @ 4.2 K

382 A @ 2.2 K

Sextupole lop 132 A @ 1.9 K (or 40% on the load line)

- 2) To commission the “small” magnet test station, to be used to test sextupole, octupole and decapole



Test results



First test at 4.2 K

Current increased by steps at 0.3 A/s. Quench induced with heaters at 90, 160, 200 and 220 A. Ramp up to 260 A (no quench induced at this current value by choice).

No spontaneous quench occurred.

Test at subcooled LHe

Significant heat load in the bath prevents from reaching a temperature lower than 2.5 K. Main reason is the thermal shield, whose temperature decreases very slowly: T_{shield} 194 K (early morning Apr 15), 134 K (night between Apr 16 and 17).

Current ramp up to quench.

Four training quenches occurred at

295 A (2.56 ± 0.04 K) or 80% of the s.s. at this T

318 A (2.60 ± 0.04 K) or 87% "

329 A (2.72 ± 0.05 K) or 91% "

325 A (2.85 ± 0.06 K) or 91% "

Training at 4.2 K

Current ramp up to quench at 0.3 A/s

First quench at 280 A, then repeated increasing the ramp rate up to 5.7 A/s (limited by power supply in this configuration). In total **14 quenches at 280 A** (or 95% of the s.s. limit).

*(caveat: in the FEM model of the single coil I do not use infinite elements
-> overestimated peak field on the coil -> underestimated short sample limits)*

6. Next Steps & Planning



Winding and impregnation tooling/mould **manufactured**

Tooling teflon coating **mid June**

Winding & Impregnation of six coils **mid September** (considering vacations)

Preliminary offer from workshop for components manufacture **mid June**

Components manufacture **mid September**

Magnet mechanical assembly **mid October**

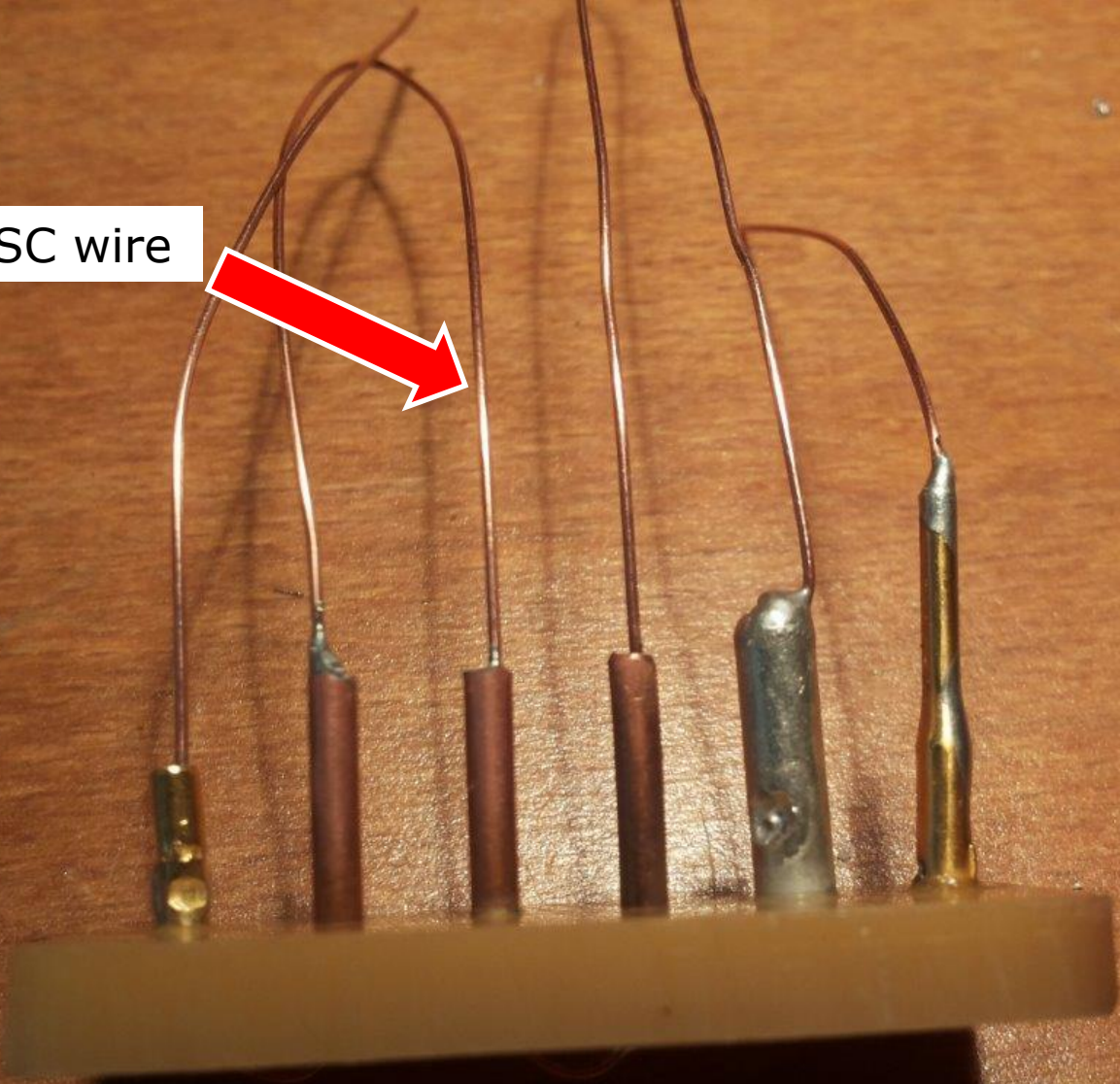
Magnet LHe tested at LASA **beginning November**

*We have hired an experienced physicist and engineer (i.e. one person with both qualifications!) to start on **Sep 1st** to collaborate to the corrector design and manufacture.*



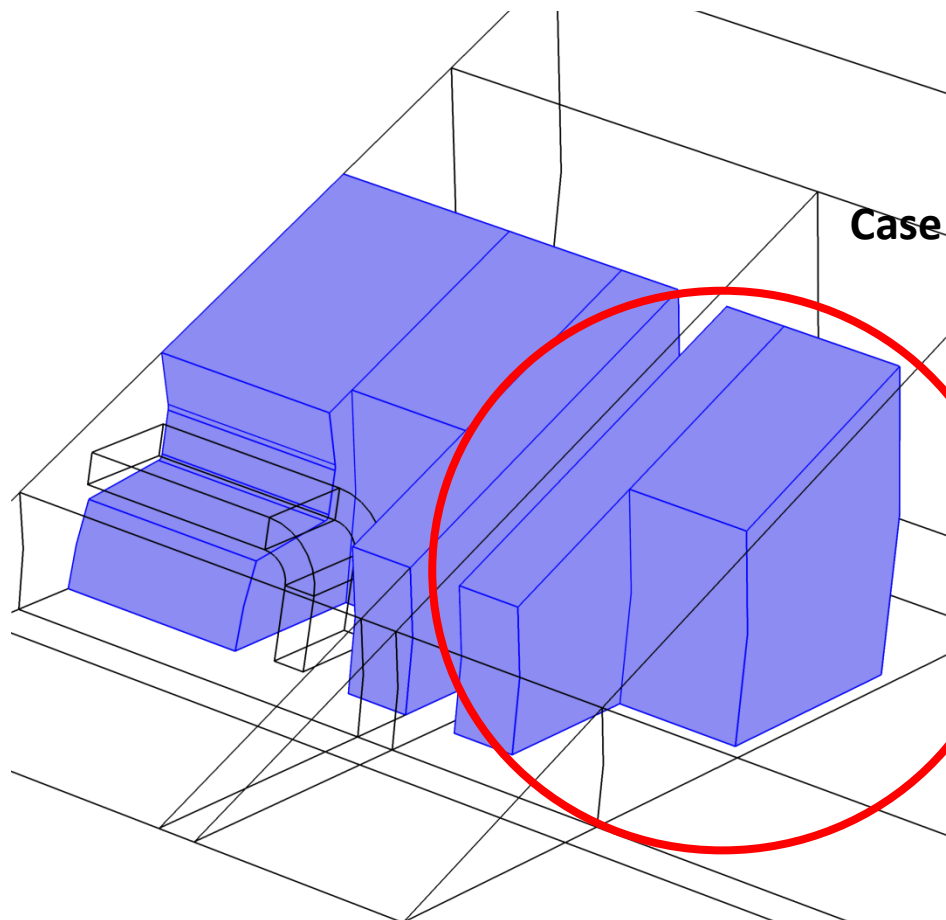
The End

0.5 mm dia SC wire

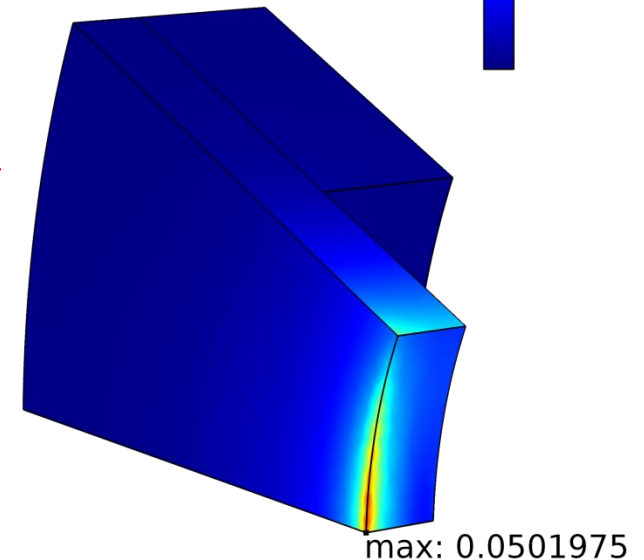
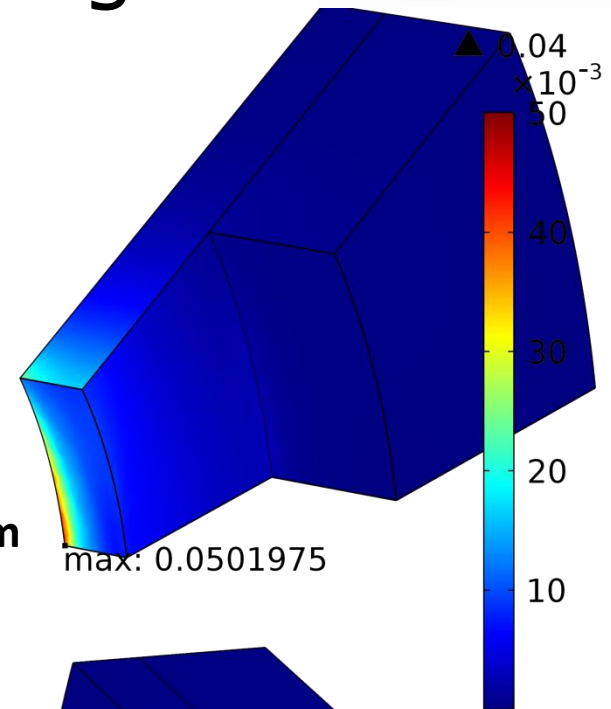


cross-talk in the coupled magnet

The magnetic induction in the FRY of the coupled magnet is mostly concentrated close to the bore, and is extremely small in the bridge connecting the FRY to the yoke (the latter is not modeled)

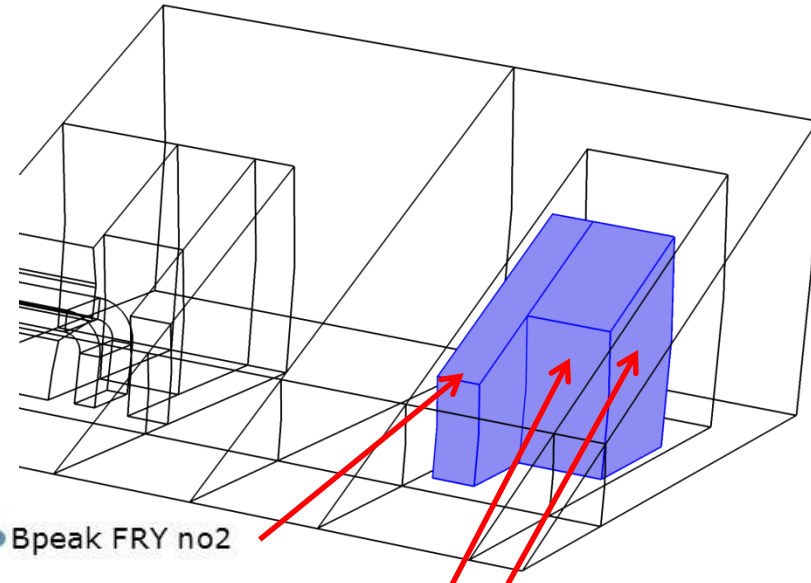


Case $d = 10$ mm

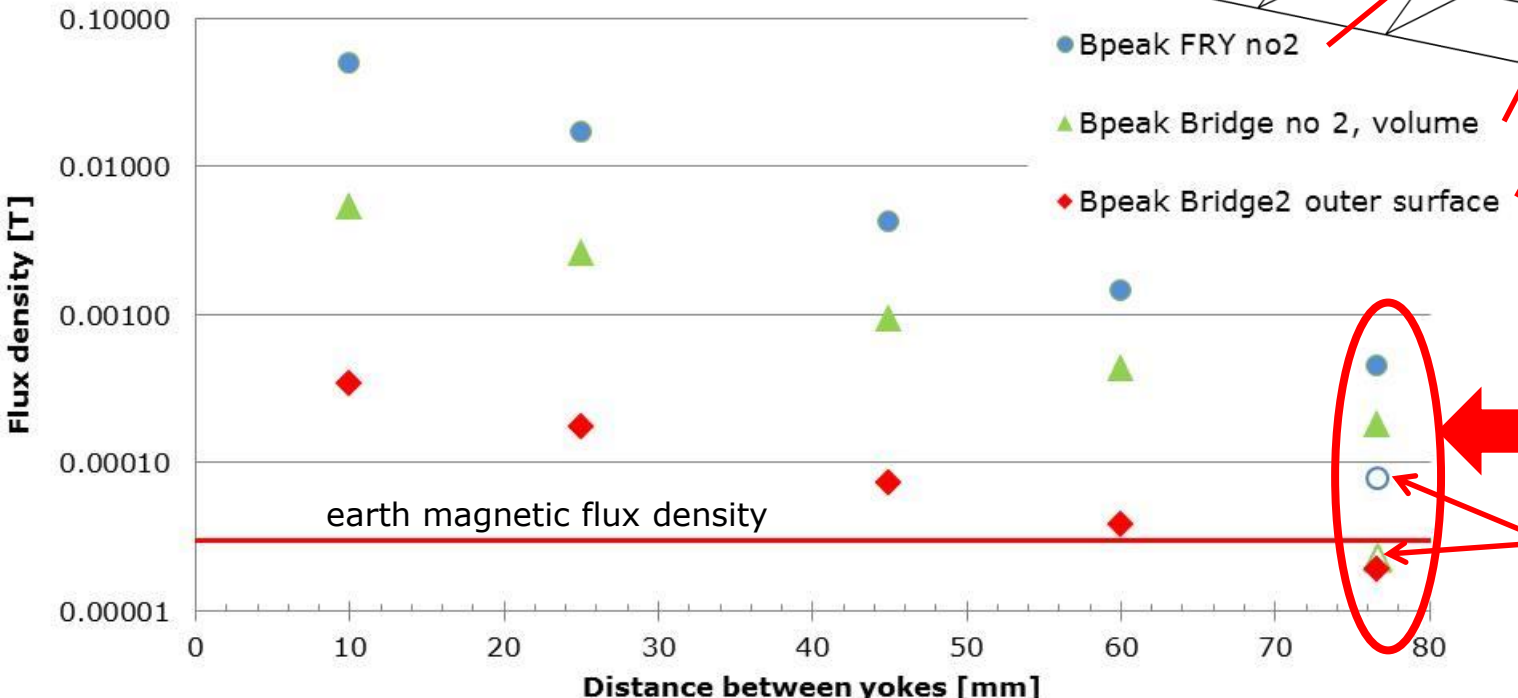


B in the coupled magnet as a function of the separation: octupole

Flux density in the coupled magnet FRY and bridge decreases exponentially with increasing separation between magnets. We can assume that the value in the yoke is even smaller, leading to a negligible excitation of the magnet.



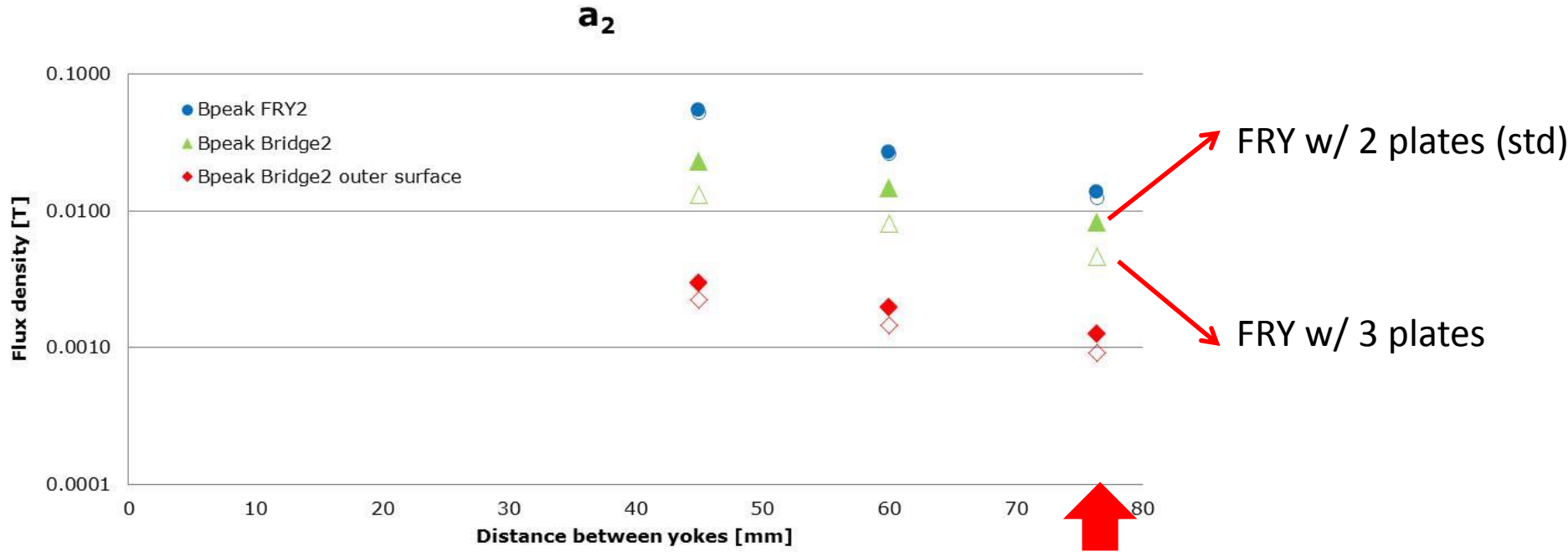
- Bpeak FRY no2
- ▲ Bpeak Bridge no 2, volume
- ◆ Bpeak Bridge2 outer surface



Nominal separation between iron yokes: 76.44 mm

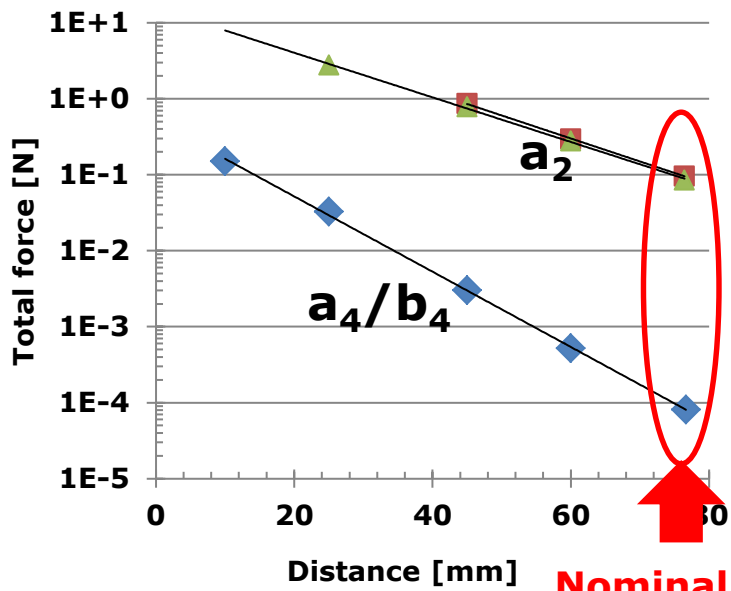
Cross check: Iron replaced w/ air in the second magnet

B in the coupled magnet as a function of the separation: quadrupole



Nominal separation
between iron yokes:
76.44 mm

Forces between magnets



Attractive force decreases exponentially, the higher orders the faster.

$$F(z) = F(0) e^{-z/\lambda}$$

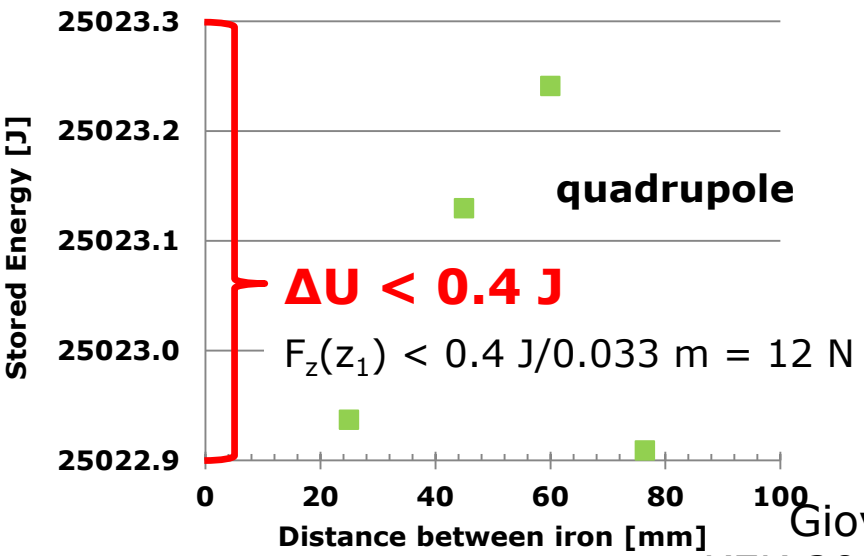
- $\lambda \approx 33$ mm (quadrupole)
- $\lambda \approx 20$ mm (octupole)

If ΔU is an upper bound for the stored energy variation changing the separation by $\Delta z = z_2 - z_1$, an upper bound for the attractive force is given by

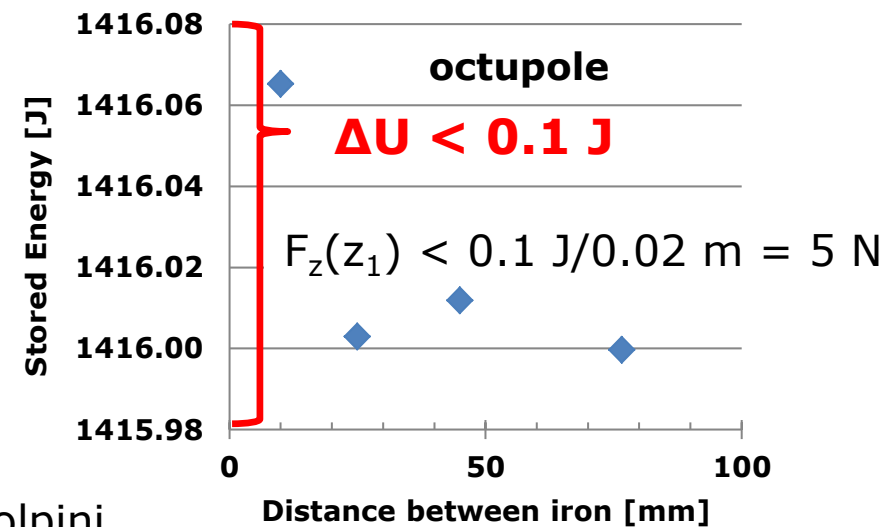
$$F(z_1) < \Delta U / \lambda \quad ; \quad \lambda < \Delta z$$

$$F(z_1) < \Delta U / \Delta z \quad ; \quad \lambda > \Delta z$$

Nominal separation between iron yokes: 76.44 mm



$\Delta U < 0.4$ J
 $F_z(z_1) < 0.4 \text{ J} / 0.033 \text{ m} = 12 \text{ N}$



octupole
 $\Delta U < 0.1$ J
 $F_z(z_1) < 0.1 \text{ J} / 0.02 \text{ m} = 5 \text{ N}$